European Journal of Medicinal Chemistry 47 (2012) 299–311

Contents lists available at SciVerse ScienceDirect

European Journal of Medicinal Chemistry

journal homepage: http://www.elsevier.com/locate/ejmech

Original article

Disubstituted quinazoline derivatives as a new type of highly selective ligands for telomeric G-quadruplex DNA

Zeng Li, Jia-Heng Tan, Jin-Hui He, Yi Long, Tian-Miao Ou, Ding Li*, Lian-Quan Gu, Zhi-Shu Huang*

School of Pharmaceutical Sciences, Sun Yat-sen University, Guangzhou 510006, People's Republic of China

ARTICLE INFO

Article history:
Received 23 September 2011
Received in revised form
25 October 2011
Accepted 28 October 2011
Available online 7 November 2011

Keywords:
Quinazoline derivatives
G-quadruplex DNA
Interaction
Selectivity
Telomerase inhibition

ABSTRACT

A series of 2,4-disubstituted quinazoline derivatives found to be a new type of highly selective ligand to bind with telomeric G-quadruplex DNA, and their biological properties were reported for the first time.Their interactions with telomeric G-quadruplex DNA were evaluated by using fluorescence resonance energy transfer (FRET) melting assay, circular dichroism (CD) spectroscopy, surface plasmon resonance (SPR), nuclear magnetic resonance (NMR), and molecular modeling. Our results showed that these derivatives could well recognize G-quadruplex and have high selectivity toward G-quadruplex over duplex DNA. The structure–activity relationships (SARs) study revealed that the disubstitution of quinazoline and the length of the amide side chain were important for its interaction with the G-quadruplex. Furthermore, telomerase inhibition of the quinazoline derivatives and their cellular effects were studied.

1. Introduction

Human nucleic acid sequences containing multiple close segments of three or more consecutive guanosine residues can form higher-order and functionally useful structures called the G-quadruplexes [1–3]. They are a type of particular secondary structure that originates in the assembly of four G-rich DNA strands held together via the formation of a G-quartet [3,4]. Such motifs have been identified in biologically relevant regions of the eukaryotic genome, particularly enriched in telomeric regions [5,6], insulin-linked polymorphic region [7], regulatory sequences of muscle-specific genes [8], and upstream of transcription initiation sites of proto-oncogenes [9–12]. This finding was the initial paradigm to search for small molecules that have the ability to stabilize G-quadruplex in order to control gene expression and reverse tumor cell immortalization [13,14]. Many groups have reported their results targeting G-quadruplex nucleic acids with small molecules as antitumor agents, since they could inhibit telomerase activity and interfere with telomere biology, or alter G-quadruplex related gene expression, or inhibit rRNA biogenesis in most cancer cells but not in normal cells [15–18]. Numerous G-quadruplex binders have been reported, and most of these molecules comprise a planar, aromatic core presumed to stack on the terminal tetrads of G-quadruplex. Examples include polyaromatic hydrocarbons and macrocyclic frameworks, which have exhibited a strong G-quadruplex stability [19–26]. Besides these compounds, some flexible ligands with unfused aromatic scaffold have aroused wide interest recently because of their adaptive structural feature arising from the rotatable bonds, which prevent the ligands from intercalating into duplex DNA but can still allow the ligands to stack on the G-quartet [14,27–33]. On the basis of above results, the introduction of a moiety as a switch to control the transformation of the ligand between the rigidity and flexibility is a new strategy in G-quadruplex ligands design.

Previous studies have shown that the moiety of intramolecular hydrogen bond is one of the most important chemical interactions that form active structures/foldings of molecules and provide critical functions in medicinal chemistry [34–36]. The beneficial effect of intramolecular hydrogen bond on ligand-receptor binding can be rationalized with conformational restriction in which the small molecular substituents are favorably aligned with the protein pockets. The improved potency of caspase-1 inhibitors have been reported through rigidifying the molecules with an intramolecular hydrogen bond [37]. The increased binding affinity and

Abbreviations: FRET, fluorescence resonance energy transfer; CD, circular dichroism; SPR, surface plasmon resonance; NMR, nuclear magnetic resonance; TRAP, telomere repeat amplification protocol; MTT, methyl thiazolyl tetrazolium; SA-β-Gal, senescence-associated-galactosidase; TRF, telomeric restriction fragment.

* Corresponding authors. Tel./fax: +86 20 39943056.
E-mail addresses: liding@mail.sysu.edu.cn (D. Li), ceshzs@mail.sysu.edu.cn (Z.-S. Huang).

0223-5234/$ – see front matter © 2011 Elsevier Masson SAS. All rights reserved.
doi:10.1016/j.ejmech.2011.10.057

pharmacological activity have also been observed for aldose reductase inhibitors by utilizing an intramolecular hydrogen bond to position the key structural elements of the pharmacophore in a certain conformation [38]. In addition, rational design of internal hydrogen bonds for conformational preorganization has been pursued in scaffold replacements for a diverse set of kinase inhibitors, such as 4-aminoquinazoline scytalone dehydratase inhibitors [39], anthranilamide kinase inhibitors [40], pyrimidin-4-ylurea kinase inhibitors [41], and alkoxybenzamide poly(ADP-ribose) polymerase inhibitors [42].

On the other hand, isaindigotone derivatives have been developed in our lab as selective telomeric G-quadruplex binding ligands [33]. Recent studies suggest that the decreased planarity of the flexible ligands would result in their decreased binding affinity and stabilization ability [43]. So a planar central core may be essential for the binding of ligand with the G-quadruplex. And the intramolecular hydrogen bond as one important moiety could rigidify the molecules and maintain a planar structure. Based on these discoveries, we designed and synthesized a series of 2,4-disubstituted quinazoline derivatives conformationally constrained with intramolecular hydrogen bonds as a new type of G-quadruplex binding ligands (Scheme 1). The internally organized hydrogen bond is positioned between the NH group at the *ortho*-position of the benzene ring and the lone pair electrons of nitrogen in pyrimidine ring. This could give a flexible scaffold, which can prevent ligand from intercalating into the duplex DNA. It could also provide a coplanar conformation of the main core, which allows ligand to effectively stack on the G-quartet. Therefore, the ligand's quadruplex binding affinity and selectivity may be all improved. However, based on previous reports [44], we hypothesized that the scaffold of quinazoline itself alone is probably not a sufficiently to be an effective G-quadruplex ligand. The addition of two cationic side chains to the quinazoline parent core, which could interact with the grooves and loops of the G-quadruplex, may be necessary to enhance its G-quadruplex binding potency and selectivity, as well as its aqueous solubility. The interactions of above-mentioned ligands with telomeric G-quadruplex DNA were examined using the fluorescence resonance energy transfer-melting (FRET-melting) method, surface plasmon resonance (SPR), circular dichroism spectroscopy (CD), and the ligand–quadruplex interactions and binding modes were investigated using NMR and molecular modeling. In addition, their inhibitory effects on telomerase activity were studied using TRAP-LIG, and their cellular effects were evaluated through the measurement of cell senescence and telomere shortening.

2. Chemistry

The facile synthetic pathway for quinazoline derivatives is shown in Scheme 1. The synthetic methodology commenced with the synthesis of acylchloride through the chlorination of 4-chloro-2-nitrobenzoic acid, followed with its amidation using anthranilamide and triethylamine to give the uncyclized amide intermediates **2** [45]. Subsequently, compound 2-(4-chloro-2-nitrophenyl)-3*H*-quinazolin-4-one **3** was prepared through the oxidative ring closure of compound **2** under basic conditions, using potassium hydroxide and ethanol, with excellent yield and purity [46]. The chlorination of **3** with excess phosphorus oxychloride was carried out to give compound **4** [47]. Coupling of 3-aminopropyl-dimethylamine with 4-chloroquinazoline intermediate **4** in THF at 66 °C, afforded compound **5**. In order to obtain the amine functionality, attempts were made using the conventional procedure for the reduction of the nitro group with 80% hydrazine hydrate in the presence of 10% Pd/C and isopropanol as a solvent, which furnished amino-substituted compound **6** at 96% yield [48]. A significant feature of this reaction was that product isolation could be facilitated through the development of workup procedures without purification using chromatography. Reaction of amine **6** with acylchloride and potassium carbonate in dichloromethane gave compounds **7**–**9** at 69–85% yield. Finally, the target compounds **10a**–**10i**, **11a**–**11e**, **12a**, **12d**, and **12e** were obtained through

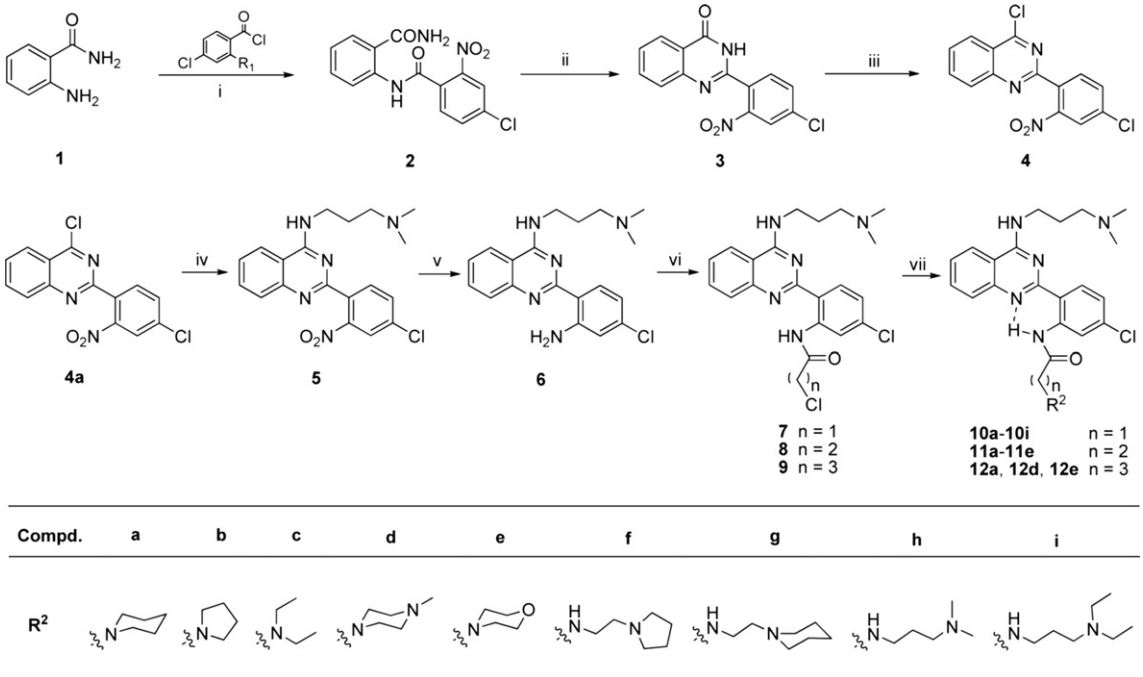

Scheme 1. Synthesis of quinazoline derivatives. Reagent: (i) 2 equiv of TEA, $CHCl_3$, rt, 5 h; (ii) 10% aqueous KOH, EtOH, reflux, 2 h; (iii) *N*,*N*-diethylaniline, $POCl_3$, toluene, reflux, 6 h; (iv) 3-aminopropyldimethyl- amine, THF, reflux, 5 h; (v) 10% Pd/C, 80% $N_2H_4H_2O$, isopropanol, reflux, 2 h; (vi) $Cl(CH_2)_nCOCl$, K_2CO_3, CH_2Cl_2, rt, 24 h; (vii) R_2NH, KI, ethanol, reflux.

aminolysis of the compounds **7**, **8**, and **9** under reflux through the treatment with the appropriate primary and secondary amines.

The ^{1}H NMR chemical shifts of acylamide protons of all the ligands in $CDCl_3$ are in the range of δ 13.51–14.12 ppm, which indicate a relatively strong intramolecular H-bonding [49–51]. In order to determine how the intramolecular hydrogen bond affect the folded state of the molecule, we performed molecular modeling experiment for compound **10h** using the semi-empirical method including a solvent model, followed with 1D selective NOESY and 2D NOESY (Figure S1). In the 1D selective NOESY experiment, upon the irradiation of proton 17-H of **10h**, only the enhancement of the equivalent protons 3-H and 13-H was observed. The cross-peak, between 17-H and 3-H, was observed on both 2D NOESY and 1D selective NOESY spectra. All these results suggested the formation of intramolecular hydrogen bond between the acylamide-NH and the pyrimidine-N7 atoms. Based on molecular modeling experiment, compound **10h** adopts a Z-shaped coplanar conformation as shown in Fig. 1.

3. Results and discussion

3.1. Studies of the stabilization and selectivity of the synthetic ligands to telomeric G-quadruplex with FRET assays

The stabilization and selectivity of the quinazoline derivatives to G-quadruplex DNA were evaluated using an FRET melting assay [52], with our previously reported quindoline derivative **SYUIQ-5** as a reference compound [53]. In order to study the selectivity of these compounds for G-quadruplex DNA over duplex DNA, a duplex oligomer ds26 was used in the present study [28,54].

Table 1 shows the effect of derivatives on the enhanced melting temperature (ΔT_m) of two labeled oligonucleotides in K^+-containing solution. F21T (5′-FAM-d(GGG[TTAGGG]$_3$)-TAMRA-3′) represents the human telomeric DNA sequence, while F10T (5′-FAM-dTATAGCTATA-HEG-TATAGCTATA- TAMRA-3′) is a hairpin duplex DNA. A comparison of the FRET assay results for the reference compound **SYUIQ-5** with fused polycyclic system and synthesized quinazoline derivatives revealed that all these ligands had high selectivity towards G-quadruplex DNA, and most of these compounds had much stronger stabilizing ability to the telomeric G-quadruplex than **SYUIQ-5**. Moreover, these derivatives had weak effect on the thermal stability of the duplex DNA F10T (Table 1, $\Delta T_m < 1$ °C), implied that these derivatives were not duplex DNA-binding ligands [29].

Table 1
Stabilization temperatures (ΔT_m) determined with FRET experiment.[a]

Compound	F21T (ΔT_m/°C)	F10T (ΔT_m/°C)	Compound	F21T (ΔT_m/°C)	F10T (ΔT_m/°C)
10a	5.4 ± 0.6	0.2 ± 0.0	**11b**	12.8 ± 0.5	0.2 ± 0.1
10b	7.4 ± 0.5	0.1 ± 0.1	**11c**	14.4 ± 0.4	0.1 ± 0.1
10c	4.5 ± 0.6	0.1 ± 0.0	**11d**	15.5 ± 0.6	0.3 ± 0.0
10d	10.1 ± 0.3	0.3 ± 0.1	**11e**	8.4 ± 0.6	0.1 ± 0.1
10e	3.9 ± 0.7	0.0 ± 0.0	**12a**	11.6 ± 0.3	0.2 ± 0.0
10f	10.4 ± 0.8	0.3 ± 0.1	**12d**	14.7 ± 0.8	0.4 ± 0.1
10g	9.6 ± 0.4	0.2 ± 0.1	**12e**	9.8 ± 0.6	0.1 ± 0.1
10h	13.0 ± 0.9	0.3 ± 0.1	**6**	0.7 ± 0.3	0.3 ± 0.1
10i	12.3 ± 0.7	0.2 ± 0.1	**SYUIQ-5**	9.9 ± 0.5	5.5 ± 0.1
11a	11.8 ± 0.7	0.2 ± 0.1			

[a] The melting point of native DNA quadruplex was 60 °C ΔT_m, change in melting temperature at 1 μM compound concentration and 200 nM DNA concentration.

The different derivatives were found to have varying effect in stabilizing the telomeric G-quadruplex. A comparison of the FRET assay results indicated that existence and the length of the amide side chain at the *ortho*- position of the aromatic group had a significant effect. The intermediate **6** without the amide side chain didn't show any effect on G-quadruplex stability. With the same basic terminus, compounds **11a**–**11e** with longer side chains ($n = 2$, with three bonds between basic N terminus and carbonyl group) showed stronger affinity to the telomeric G-quadruplex than compounds **10a**–**10e** with shorter side chains ($n = 1$, with two bonds between basic N terminus and carbonyl group), while no distinct effect on ΔT_m values was observed with the further extension of amide side chain, as shown for compounds **12a**, **12d**, **12e**, and **10f**–**10i**, with four or five bonds between basic N terminus and carbonyl group. On the other hand, alterations of the basic terminus of the amide side chains showed that the *N*-methyl piperazino analogues (**10d**, **11d** and **12d**) had strongly enhanced affinity for G-quadruplex DNA over the piperidino, pyrrolidino, and diethylamino analogues, with the less basic morpholino analogues (**10e**, **11e** and **12e**) proving detrimental to G-quadruplex affinity. These results demonstrated the importance of length and basicity of amide side chain for strong G-quadruplex interactions.

Furthermore, the selectivity of these derivatives to G-quadruplex was assessed with an FRET-based competition assay, and the ability of the ligand to stabilize G-quadruplex was challenged with nonfluorescent duplex DNA (ds26, 5′-CAATCGGATCGAATT-CGATCCGATTG-3′) [28,55]. In the presence of varying amount of competitor ds26, the thermal stabilization of F21T enhanced by

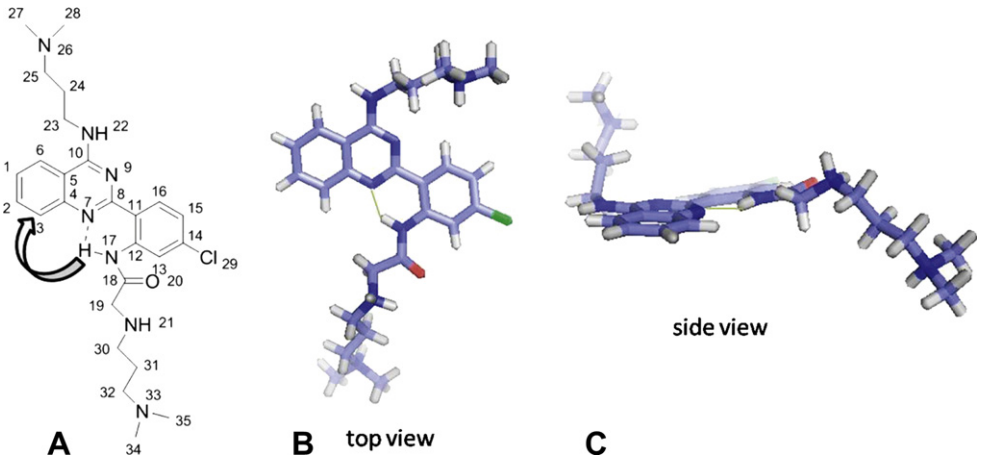

Fig. 1. Structure of **10h** (A); energy minimized structures (Chem 3D Ultra 10.0, CambridgeSoft Corp, MA) of **10h**, at side view (B) and bottom view (C). The NOE cross peaks are indicated with arrow. A intramolecular hydrogen bond was marked as dash line in A and green line in B. (For interpretation of the references to colour in this figure legend, the reader is referred to the web version of this article.)

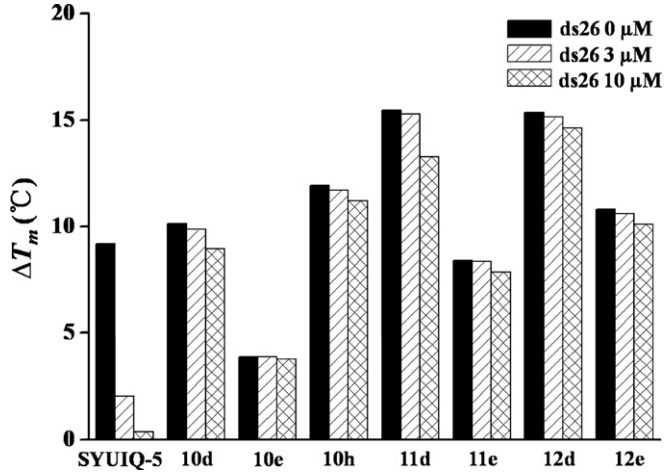

Fig. 2. Competitive FRET results for **SYUIQ-5** and ligands **10d**, **10e**, **10h**, **11d**, **11e**, **12d**, and **12e** (1 μM), without and with excess of duplex DNA competitor (ds26). The concentrations of ds26 were 0, 3, 10 μM.

some selected compounds was slightly affected (Fig. 2), while the competitor significantly disrupted the binding of **SYUIQ-5** to the G-quadruplex. Our above experimental results demonstrated that unfused quinazoline derivatives were found to be a new type of highly selective human telomeric G-quadruplex binding ligands.

3.2. Studies of binding and selectivity of the synthetic ligands to telomeric G-quadruplex with surface plasmon resonance (SPR)

SPR is a useful technique to monitor molecular reactions in real time, which has been applied to investigate the interactions between small molecular ligands and human G-quadruplex DNA [55,56]. Here, SPR experiments were carried out in order to quantitatively determine the kinetic constants of the quinazoline derivatives binding to either G-quadruplex or duplex DNA. Figure S4 show the SPR sensorgrams of **10d**, **10h**, **11d**, and **12d** binding to the immobilized telomeric G-quadruplex (HTG21, 5′-d(GGG[TTAGGG]$_3$)-3′) at different concentrations. Then K_D was calculated by global fitting of the kinetic data from various concentrations of quinazoline derivatives using Langmuir binding model (Table 2). As the data shown, The binding constants of the disubstituted compounds to telomeric G-quadruplex showed strong binding affinity (K_D, 0.337–2.11 μM), while no obvious binding was observed using SPR for mono substituted compound **6** even at a concentration of 20 μM, which was consistent with very low ΔT_m values obtained from FRET melting. These results further confirmed the importance of the disubstitution for the binding of quinazoline derivatives to the telomeric G-quadruplex.

Table 2
Kinetic parameters determined with SPR spectroscopy.[a]

	k_a (M^{-1} s^{-1})		k_d (s^{-1})		K_D (M)	
	Htelo[b]	Duplex[c]	Htelo[b]	Duplex[c]	Htelo[b]	Duplex[c]
10d	4.26×10^4	_[d]	0.09	_[d]	2.11×10^{-6}	_[d]
10h	2.76×10^5	_[d]	0.05	_[d]	3.37×10^{-7}	_[d]
11d	2.83×10^5	_[d]	0.09	_[d]	3.14×10^{-7}	_[d]
12d	2.52×10^5	_[d]	0.07	_[d]	2.78×10^{-7}	_[d]

[a] k_a is association constant, while k_d is dissociation constant. K_D denotes the equilibrium dissociation constant, given by k_d/k_a.
[b] Htelo (Quadruplex): 5′-biotin-[(GTTAGG)$_5$]-3′.
[c] Duplex: 5′-biotin-T$_9$CGAATTCGT$_5$CGAATTCG-3′.
[d] No significant binding was found for addition of up to 10 or 20 μM ligand. IC_{50}.

Both FRET and SPR experimental results indicated that the amide side chains of the tested compounds with at least three bonds between basic N terminus and C═O bond of amide group (**10h**, **11d**, **12d**) were optimal for their interactions with telomeric G-quadruplex DNA. For the study of their binding selectivity for quadruplex over duplex by SPR, incubation of these compounds with duplex DNA immobilized on the chips showed neither significant nor specific binding interactions, which prevented the determination of their binding affinity (Figure S5). This might indicate that these disubstituted quinazoline derivatives had good selectivity for G-quadruplex DNA, which was in agreement with the FRET data.

3.3. Studies of the binding property of the synthetic ligands to telomeric G-quadruplex with circular dichroism (CD)

CD spectroscopy is a highly sensitive method for determining the conformation of G-quadruplex structures and the effect of ligand binding on quadruplex structure [57]. The binding property of the disubstituted quinazoline derivatives to telomeric G-quadruplex was further studied with this method. It has been reported that HTG21 has formed a hybrid-type of quadruplex DNA containing parallel and anti-parallel structure in the presence of K^+, with a large positive band at 290 nm, a shoulder at around 270 nm, a small positive band at 255 nm, and a minor negative band near 234 nm on CD spectra [56,57]. In the present study, upon the addition of compound **11d** to the above solution, the CD spectrum significantly changed, with a maximum band at 290 nm increased and shifted toward 286 nm, and the shoulder at 270 nm gradually enhanced and merged into the band at 286 nm. Meanwhile, the small positive band at 255 nm gradually disappeared and led to the appearance of a positive band at 240 nm and a major negative band at 260 nm (Fig. 3A). Compound **11h** and **12d** induced similar CD changes (Figure S6). However, dramatically different changes in the CD spectra were observed when the compound **10d** was titrated into the HTG21 oligonucleotide in the presence of K^+. Addition of **10d** resulted in stronger intensities of both the positive band at 290 nm and the shoulder at around 270 nm, and only a remarkable attenuation of the band at 255 nm (Fig. 3B). These results are consistent with those obtained from other experiments in the present study, and may further support the results of the thermodynamic stability studies indicating the importance of amide side chain length for strong G-quadruplex interactions. Also, all of above changes were obviously concentration dependent, but we were not able to figure out particular conformational changes occurring for HTG21 based on the present information.

3.4. Studies of the binding property of the synthetic ligands to telomeric G-quadruplex with ^{1}H NMR

In order to further investigate the binding affinity and binding models between quinazoline derivatives and G-quadruplex at a molecular level, we carried out ligand titration experiments with an intermolecular four-stranded parallel G-quadruplex DNA formed from [d(TTAGGG)]$_4$ (HT-6) [58,59], a single repeat sequence of the human telomere, followed with analysis using ^{1}H NMR.

Based on the 1D selective NOESY and 2D NOESY studies mentioned above, the intramolecular hydrogen bond between the acylamide-NH and the pyrimidine-N7 atoms of the quinazoline derivatives was formed in $CDCl_3$. To explore the structural state of the compound **11d** in the experimental solution, ^{1}H NMR studies in K^+-containing buffer using a pH Gradient Method was carried out. As shown in Figure S7, the ^{1}H NMR spectrum of **11d** in K^+-containing buffer revealed that the signal of an acylamide proton at δ 15.65 ppm still exist at pH 4.0, which indicated intramolecular

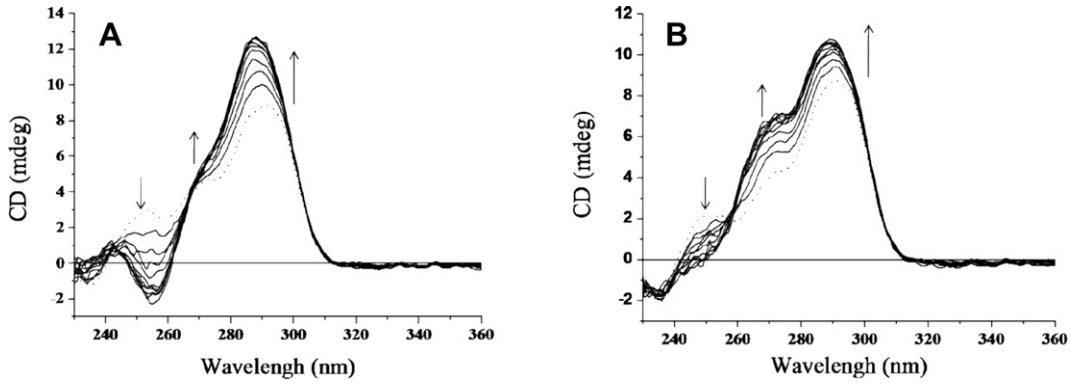

Fig. 3. CD titration spectra of HTG21 (5 μM) at increasing concentrations of **11d** (A) and **10d** (B) (arrows: 0–5 Mol equiv; dashed line indicated HTG21 in the absence of ligands) in 10 mM Tris–HCl buffer, pH 7.2, with 100 mM KCl.

hydrogen bond would keep a steady state during the NMR experiments.

In the titration experiments, both downfield- and upfield-shifted portions of 400 MHz ^{1}H NMR spectrum of $[d(TTAGGG)]_4$ at 25 °C were observed in the absence of compound **11d** as shown in Fig. 4. The imino proton signals attribute to G4-G6 were resolved in the downfield-shifted region (10–12 ppm). The binding of **11d** to the $[d(TTAGGG)]_4$ was confirmed by a general line-broadening of the $[d(TTAGGG)]_4$ resonance signals upon addition of the ligand [60]. There were marked upfield shifts in the imino proton region of the $[d(TTAGGG)]_4$, indicative of π–π interactions between the aromatic surface of the ligand and the terminal G-tetrad(s) of the $[d(TTAGGG)]_4$ [60]. Interestingly, at a ratio of 0.5:1 for ligand:quadruplex stoichiometry, another set of new proton signal was observed in the downfield (δ = 14.51 ppm), which became dominant at increasing ligand concentration. These results demonstrated that the intramolecular hydrogen bond of the ligand still remained in the process of the interaction between quinazoline derivatives and G-quadruplex DNA. Besides, for a number of proton resonance signals from the aromatic nucleobases (A3: H8, H2; G4: H8), the line-broadening changes started to level with an increasing **11d** concentration, suggesting that **11d** binds to $[d(TTAGGG)]_4$ near the A3 and G4 residues, and demonstrating that the time scale for the formation of the complex of **11d** and $[d(TTAGGG)]_4$ is faster than the ^{1}H NMR time scale. In summary, these data support that the ligands bind to and stabilize the G-quadruplex formed by the $[d(TTAGGG)]_4$.

3.5. Molecular modeling studies

Molecular docking experiments were performed on some of ligand-G-quadruplex complexes to investigate the best binding mode between the G-quadruplex and the quinazoline derivatives. Compound **11d** was selected for this study as one of the best binding ligands. The crystal structure of the mixed hybrid-type telomeric G-quadruplex ($d[AG_3(T_2AG_3)_3]$, PDB code: 2HY9 [61,62]) with potassium ion was used as the starting point for the modeling because it might be a more biologically relevant form. The hybrid-type G-quadruplex conformation, with its 5′- and 3′-ends pointing to opposite directions, can provide an efficient scaffold for the formation of compact-stacking multimer structures in the human telomeric DNA. Our results showed that quinazoline derivatives could stack on both external G-quartet planes. In this experiment, 100 random starting structures were generated, and 28 structures with lowest energy (average intermolecular binding energy, ΔG = −11.72 kcal/mol) were obtained after the docking protocol were analyzed for **11d** (Fig. 5A). As shown in Fig. 5B, preferable binding site of **11d** was found to be 5′-terminal G-quartet plane (with an edgewise loop) for 2HY9. The aromatic core with a planer "imitative" tetracyclic structure formed through intramolecular hydrogen bond (2.6 Å) stacks on at least two guanines with its side chains in adjacent grooves. The ligand had three to four hydrogen bonds with either guanine nitrogen or backbone oxygen atoms, contributing to the stabilization of the complex. This is consistent with thermal stability of G-quadruplex in the presence of these quinazoline derivatives, which is attributed to the stable hydrogen bondings, π–π stacking interactions, and electrostatic interactions.

The combinations of NMR experimental results and molecular modeling studies indicated that both intramolecular hydrogen bond and π–π stacking interaction with G-quartet may maintain the planarity of the aromatic region in **11d** during its interaction with G-quadruplex DNA. G-Quartets are derived from the association of four guanines into a cyclic Hoogsteen hydrogen-bonding arrangement with two hydrogen bonds between two adjacent guanine bases, which supplied a lager square aromatic surface than

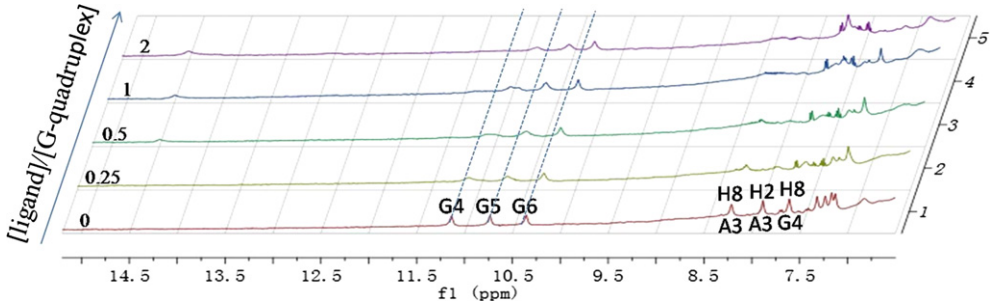

Fig. 4. ^{1}H NMR spectra (400 MHz) of $[d(TTAGGG)]_4$ for which $R_{\mathbf{11d}}${[**11d**]/[$[d(TTAGGG)]_4$]} = 0, 0.25, 0.5, 1 and 2 in 0.5 mM $[d(TTAGGG)]_4$, 25 mM potassium phosphate buffer (pH 7.0), and 150 mM KCl at 25 °C. Most DNA signals exhibited upfield shifts and were line-broadened with an increase in the R_{11d} value. The assignments of some signals are given in the spectra.

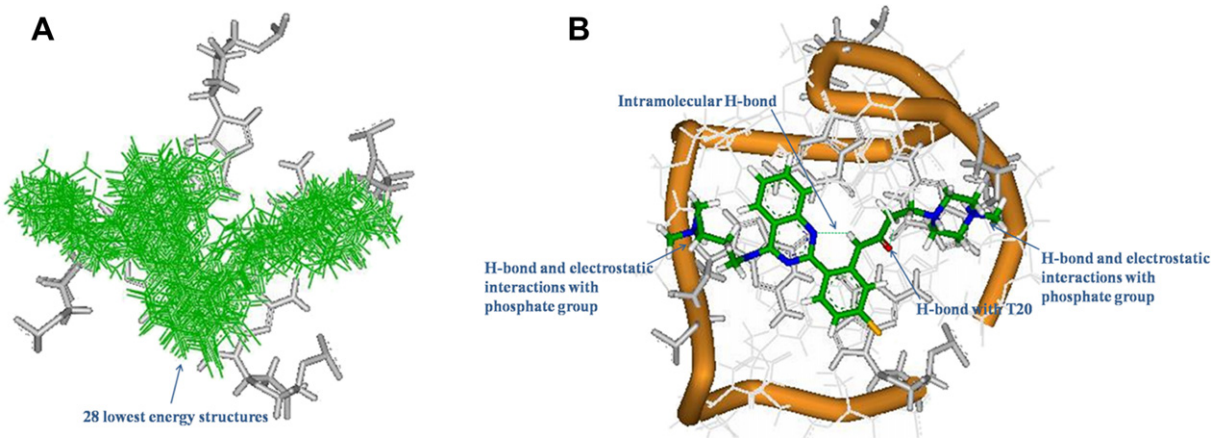

Fig. 5. Results of the docking calculation showing **11d** complexed to the 2HY9 human intramolecular quadruplex. (A) Overlay of 28 structures with the lowest energy, illustrating the unique position of the aromatic ring over the 5′-G-quartet (in Green). (B) representative structure showing **11d** and the solvent-excluded molecular surface area of the quadruplex. (For interpretation of the references to colour in this figure legend, the reader is referred to the web version of this article.)

Table 3
Telomerase inhibition by quinazoline derivatives in cell-free assay.

	10d	11d	12d
IC_{50} (μM)	29.3	7.4	7.7

the Watson-Crick base pairs of duplex DNA [1]. The formation of intramolecular hydrogen bond in **11d** could increase the area of π–π stacking of the compound and finally result in an increase of its binding affinity to G-quadruplex DNA.

3.6. Telomerase inhibition

The ability of quinazoline derivatives to inhibit human telomerase activity were evaluated by a modified TRAP assay, the TRAP-LIG assay [63]. This method provided qualitative and quantitative estimates of telomerase inhibition by the small molecules. Considering that the presence of the compounds in the extended products would possibly interfere with the PCR step, the ligands were removed prior to the amplification step [64]. In the experiments, solutions of derivatives were added to the telomerase reaction mixture containing extract from cracked MCF-7 breast carcinoma cell lines, and the inhibitory concentrations by half values ($^{Tel}IC_{50}$) of these compounds are listed in Table 3. It was found that the inhibitory effects of disubstituted quinazoline derivatives with longer amide side chain (with at least three bonds between basic N terminus and C═O bond of amide group) on telomerase activity were significantly enhanced when compared to that of the shorter one **10d**. In general, a good correlation was found between G-quadruplex stabilization potency and telomerase inhibition among quinazoline derivatives synthesized.

3.7. Senescence induced by quinazoline derivative *11d*

Since compound **11d** was found to be one most promising compound as a telomerase inhibitor and telomeric G-quadruplex binding ligand in the above studies, the following further in-depth

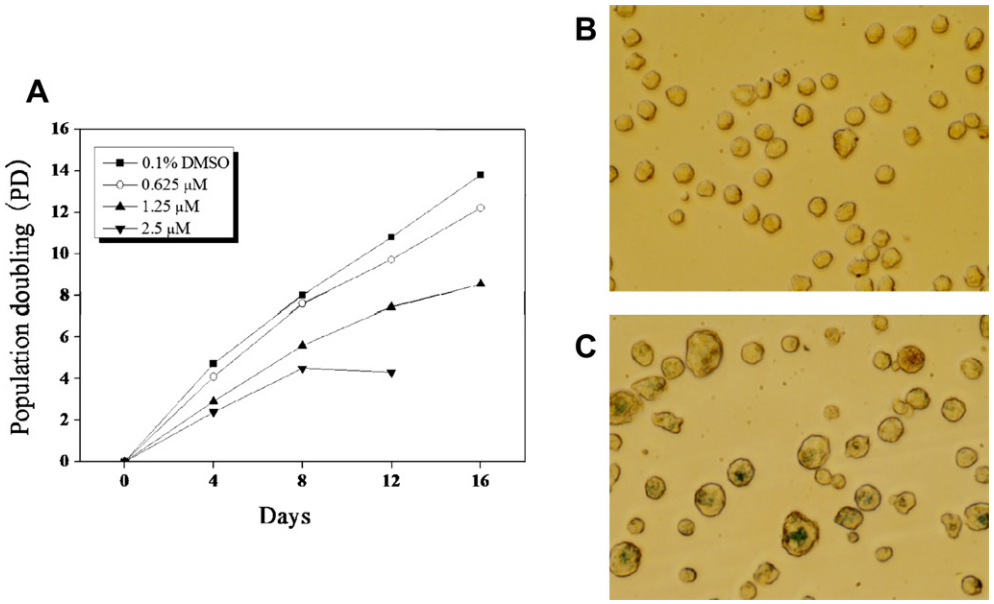

Fig. 6. Senescence induced by compound **11d** on HL60 cells. (A) Long-term incubation of HL60 with compound **11d** at subcytotoxic concentrations. Expression of SA-β-Gal in HL60 cells after treatment with (B) 0.1% DMSO and (C) 1.25 μM compound **11d** continuously for 16 days.

experimental studies were carried out only for this particular compound. To examine the effect of ligand **11d** on leukemia cell HL60, short-term cell viability was determined in a two-day cytotoxic assay (MTT assay) first. The results show that **11d** has a potent inhibitory effect, with an IC_{50} value of 9.6 μM.

To avoid acute cytotoxicity and other nonspecific events that could lead to difficulty in result interpretation, subcytotoxic concentrations (0.625, 1.25 and 2.5 μM) of **11d** were evaluated on HL60 for long-term exposure. Upon treatment of HL60 cells with 2.5 μM **11d**, a significantly inhibitory effect was found after 8 days and the growth was halted after 12 days. At 1.25 μM, a delayed effect was also observed, with the number of population doublings significantly decreased after 12 days, and even with 0.625 μM **11d**, a discernible difference was observed between the control and treated cells (Fig. 6A).

Morphological examination of the cells in long-term studies showed an increased proportion of enlarged and flattened cells with phenotypic characteristics of senescence [65,66]. These flattened cells were also stained positively for the senescence-associated-galactosidase (SA-β-Gal) activity after continuous treatment with compound **11d** (Fig. 6B and C), and our result showed that compound **11d** induced accelerated senescence of HL60 cancer cells.

3.8. Telomere shortening by quinazoline derivative *11d*

Long term treatment of tumor cells at subapoptotic dosage with telomeric G-quadruplex ligands have been previously reported to disrupt telomere length maintenance and caused telomeres to erode [67]. To investigate whether representative quinazoline derivative **11d** could cause telomeres to shorten, the telomere length was evaluated using the telomeric restriction fragment (TRF) length assay (Fig. 7) on leukemia cell HL60. The results showed that 1.25 μM of **11d** triggered telomere shortening about 1.2 kb against HL60 cells, and telomere shortening was also observed after 0.625 μM of **11d** treatment. Telomere dysfunction could activate p53 to initiate cellular senescence or apoptosis to suppress tumorigenesis [25], and here the induction of senescence by compound **11d** might be due to the shortening of telomere length, which is consistent with those reported previously for efficient telomeric G-quadruplex ligands and telomerase inhibitors [68]. But we must be noted that the cellular effect of compound **11d** may not be simply explained through telomeric G-quadruplex interactions or telomerase inhibition. This molecule could also be targeted for other possible telomere-independent genomic DNAs, such as promoter G-quadruplex. Nevertheless, compound **11d** still could be considered as useful lead for anticancer approach for its optimal selectivity towards G-quadruplex DNA.

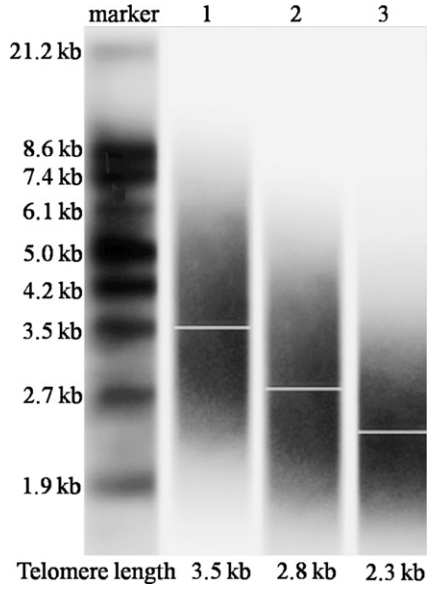

Fig. 7. Effect of quinazoline derivative **11d** on telomere length. TRF analysis of HL60 cells treated with or without compound **11d** for 16 days. Lane 1, 0.1% DMSO; lane 2, 0.625 μM compound **11d**; lane 3, 1.25 μM compound **11d**.

4. Conclusion

Rational design of molecules targeting the telomeric G-quadruplex DNA is a promising approach. On this basis, several unfused aromatic compounds were designed, synthesized, and evaluated as effective and selective telomeric G-quadruplex binding ligands. Compared with many G-quadruplex ligands with rigid or flexible structures, the compounds synthesized in the present study are novel "imitative" tetracyclic aromatic system formed through intramolecular hydrogen bond, which enable adoption of moderate twisted and coplanar conformations of the aryl groups, and allow the ligands to well stack on the G-quartet. Our experimental results show that these derivatives are a promising type of selective telomeric G-quadruplex binding ligands with strong discrimination against the duplex DNA. The introduced two positively charged side chains could participate in electrostatic and H-bonding interactions with the grooves and loops of the G-quadruplex DNA. The amide side chain attaching the terminal *N*-methyl piperazino group with at least three bonds between basic terminus and carboxyl group was proved to be optimal for G-quadruplex binding. Moreover, the disubstituted quinazoline derivatives were found to be strong telomerase inhibitors, and long-term incubation of HL60 cancer cells with compound **11d** showed a remarkable decrease of cell population accompanied with a shortening of the telomere length, which are consistent with those previously reported for effective telomerase inhibitors and telomeric G-quadruplex ligands. Such interesting results provide us with another new entry into G-quadruplex ligand design and conformation studies.

5. Experimental section

5.1. Synthesis and characterization

^1H and ^{13}C NMR spectra were recorded using TMS as the internal standard in DMSO-d_6 or $CDCl_3$ with a Bruker BioSpin GmbH spectrometer at 400 MHz and 100 MHz, respectively. Melting points (mp) were determined using an SRS-OptiMelt automated melting point instrument without correction. MS spectra were recorded on a Shimadzu LCMS-2010A instrument with an ESI or ACPI mass selective detector. Elemental analysis was carried out on an Elementar Vario EL CHNS Elemental Analyzer.

5.1.1. General aminolysis procedure: preparation of *10a–10i*, *11a–11e* and *12a*, *12d*, *12e*

To a stirred refluxing suspension of the chloride compounds **7**, **8** or **9** (0.5 mmol) and KI (0.08 g) in EtOH (15 mL) was added dropwise appropriate secondary amine (2.0 mL) in EtOH (5 mL). The mixture was stirred under reflux for 5 h, cooled to 0 °C, and diluted with distilled water. The resulting solution was filtered, washed with ether and water, and then evaporated under vacuum. The crude solid was purified by using chromatography with $CHCl_3$/MeOH/$NH_3 \cdot H_2O$ elution to afford **10a–10i**, **11a–11e** and **12a**, **12d**, **12e**.

*5.1.1.1. N-(5-Chloro-2-(4-(3-(dimethylamino)propylamino)quinazolin-2-yl)phenyl)-2-(piperidin-1-yl)acetamide (**10a**).* The compound **7** was treated with excess piperidine according to general aminolysis procedure to afford **10a**. After column chromatography with $CHCl_3/CH_3OH/NH_3\cdot H_2O$ (50:1:0.1) elution, the desired product was obtained as a white solid in 78% yield. mp 180–182 °C; ^{1}H NMR (400 MHz, $CDCl_3$): δ 13.51 (s, 1H), 9.00 (s, 1H), 8.89 (d, J = 2.2 Hz, 1H), 8.51 (d, J = 8.6 Hz, 1H), 7.99 (d, J = 8.2 Hz, 1H), 7.72 (t, J = 7.6 Hz, 1H), 7.60 (d, J = 8.0 Hz, 1H), 7.45 (t, J = 7.4 Hz, 1H), 7.12 (dd, J = 8.6, 2.2 Hz, 1H), 3.86 (dd, J = 10.2, 5.6 Hz, 2H), 3.26 (s, 2H), 2.67–2.61 (m, 2H), 2.57–2.44 (m, 4H), 2.41 (s, 6H), 1.94–1.87 (m, 2H), 1.46 (dt, J = 10.8, 5.6 Hz, 4H), 1.37–1.29 (m, 2H); ^{13}C NMR (101 MHz, $CDCl_3$): δ 170.12, 160.56, 159.41, 148.66, 140.14, 136.35, 132.17, 131.77, 128.41, 125.85, 123.76, 122.69, 121.02, 120.66, 113.84, 65.22, 59.93, 54.81, 45.50, 42.73, 25.28, 24.45, 23.84; HRMS (ESI): $(M-H)^-$ ($C_{26}H_{33}ClN_6O$) cacld 479.2326, found 479.2320; elemental analysis calcd (%) for $C_{26}H_{33}ClN_6O\cdot H_2O$: C 62.57, H 7.07, N 16.84; found: C 62.46, H 7.03, N, 16.84.

*5.1.1.2. N-(5-Chloro-2-(4-(3-(dimethylamino)propylamino)quinazolin-2-yl)phenyl)-2-(pyrrolidin-1-yl)acetamide (**10b**).* The compound **7** was treated with excess pyrrolidine according to general aminolysis procedure to afford **10b**. After column chromatography with $CHCl_3/MeOH/NH_3\cdot H_2O$ (50:1:0.1) elution, the desired product was obtained as a white solid in 74% yield. mp 174–175 °C; ^{1}H NMR (400 MHz, $CDCl_3$): δ 13.84 (s, 1H), 8.93 (s, 2H), 8.57 (d, J = 8.2 Hz, 1H), 7.92 (d, J = 7.8 Hz, 1H), 7.69 (d, J = 6.6 Hz, 1H), 7.60 (d, J = 7.6 Hz, 1H), 7.43 (t, J = 7.0 Hz, 1H), 7.12 (d, J = 8.2 Hz, 1H), 3.86 (dd, J = 10.0, 5.8 Hz, 2H), 3.43 (s, 2H), 2.68 (t, J = 7.0 Hz, 4H), 2.65–2.52 (m, 2H), 2.40 (s, 6H), 1.97–1.84 (m, 2H), 1.71 (t, J = 7.2 Hz, 4H); ^{13}C NMR (101 MHz, $CDCl_3$): δ 170.55, 160.50, 159.38, 148.72, 140.36, 136.42, 131.99, 131.76, 128.01, 125.79, 123.54, 122.66, 121.01, 120.69, 113.80, 62.22, 59.78, 54.52, 45.44, 42.53, 24.51, 23.93; HRMS (ESI): Cacld for $(M-H)^-$ ($C_{25}H_{31}ClN_6O$) requires *m/z* 465.2170, found 465.2162; elemental analysis calcd (%) for $C_{25}H_{31}ClN_6O\cdot H_2O$: C 61.91, H 6.86, N 17.33; found: C 61.88, H 6.53, N 17.38.

*5.1.1.3. N-(5-chloro-2-(4-(3-(dimethylamino)propylamino)quinazolin-2-yl)phenyl)-2-(diethylamino)acetamide (**10c**).* The compound **7** was treated with excess diethylamine according to general aminolysis procedure to afford **10c**. After column chromatography with $CHCl_3/MeOH/NH_3\cdot H_2O$ (50:1:0.1) elution, the desired product was obtained as a white solid in 81% yield. mp 170–172 °C; ^{1}H NMR (400 MHz, $CDCl_3$): δ 13.60 (s, 1H), 8.92 (d, J = 2.2 Hz, 2H), 8.53 (d, J = 8.6 Hz, 1H), 7.90 (d, J = 8.4 Hz, 1H), 7.71 (t, J = 7.2 Hz, 1H), 7.60 (d, J = 8.0 Hz, 1H), 7.43 (t, J = 7.6 Hz, 1H), 7.13 (dd, J = 8.6, 2.2 Hz, 1H), 3.86 (dd, J = 10.4, 5.6 Hz, 2H), 3.30 (s, 2H), 2.68 (q, J = 7.2 Hz, 4H), 2.65–2.55 (m, 2H), 2.40 (s, 6H), 1.90 (dd, J = 16.8, 5.8 Hz, 2H), 0.99 (t, J = 7.2 Hz, 6H); ^{13}C NMR (101 MHz, $CDCl_3$): δ 172.03, 160.53, 159.44, 148.88, 140.01, 136.26, 132.04, 131.93, 128.02, 125.71, 124.22, 122.73, 121.02, 120.86, 113.85, 59.92, 58.81, 49.09, 45.51, 42.65, 24.53, 11.64; HRMS (ESI): $(M-H)^-$ ($C_{25}H_{33}ClN_6O$) cacld 467.2326, found 467.2319; elemental analysis calcd (%) for $C_{25}H_{33}ClN_6O\cdot H_2O$: C 61.65, H 7.24, N 17.26, found: C 61.58, H 7.21, N 17.04.

*5.1.1.4. N-(5-Chloro-2-(4-(3-(dimethylamino)propylamino)quinazolin-2-yl)phenyl)-2-(4-methylpiperazin-1-yl)acetamide (**10d**).* The compound **7** was treated with excess *N*-methyl piperazine according to general aminolysis procedure to afford **10d**. After column chromatography with $CHCl_3/MeOH/NH_3\cdot H_2O$ (50:1:0.1) elution, the desired product was obtained as a white solid in 66% yield. mp 174–175 °C; ^{1}H NMR (400 MHz, $CDCl_3$): δ 13.51 (s, 1H), 8.98 (s, 1H), 8.86 (d, J = 2.2 Hz, 1H), 8.49 (d, J = 8.6 Hz, 1H), 7.95 (d, J = 8.2 Hz, 1H), 7.77–7.67 (m, 2H), 7.47 (t, J = 7.6 Hz, 1H), 7.13 (dd, J = 8.6, 2.2 Hz, 1H), 3.87 (dd, J = 10.4, 5.6 Hz, 2H), 3.31 (s, 2H), 2.72–2.67 (m, 2H), 2.67–2.51 (m, 4H), 2.46 (s, 6H), 2.40–2.24 (m, 4H), 2.12 (s, 3H), 2.01–1.91 (m, 2H); ^{13}C NMR (101 MHz, $CDCl_3$): δ 169.36, 160.52, 159.45, 148.55, 139.93, 136.37, 132.42, 131.75, 128.46, 126.01, 123.79, 122.85, 121.29, 120.67, 113.86, 64.20, 59.29, 54.15, 53.35, 45.80, 45.20, 42.04, 24.31; HRMS (ESI): $(M-H)^-$ ($C_{26}H_{34}ClN_7O$) cacld 494.2435, found 494.2421; elemental analysis calcd (%) for $C_{26}H_{34}ClN_7O\cdot H_2O$: C 60.75, H 7.06, N 19.07; found: C 60.66, H, 6.97, N 18.89.

*5.1.1.5. N-(5-Chloro-2-(4-(3-(dimethylamino)propylamino)quinazolin-2-yl)phenyl)-2-morpholinoacetamide (**10e**).* The compound **7** was treated with excess morpholine according to general aminolysis procedure to afford **10e**. After column chromatography with $CHCl_3/MeOH/NH_3\cdot H_2O$ (50:1:0.1) elution, the desired product was obtained as a white solid in 78% yield. m.p. 179–181 °C; ^{1}H NMR (400 MHz, $CDCl_3$) δ 13.67 (s, 1H), 9.09 (s, 1H), 8.88 (d, J = 2.2 Hz, 1H), 8.53 (d, J = 8.6 Hz, 1H), 7.92 (d, J = 8.2 Hz, 1H), 7.77–7.69 (m, 1H), 7.62 (d, J = 8.0 Hz, 1H), 7.46 (t, J = 7.6 Hz, 1H), 7.13 (dd, J = 8.6, 2.2 Hz, 1H), 3.86 (dd, J = 10.2, 5.6 Hz, 2H), 3.64–3.53 (m, 4H), 3.32 (s, 2H), 2.68–2.62 (m, 2H), 2.63–2.53 (m, 4H), 2.42 (s, 6H), 1.94–1.85 (m, 2H); ^{13}C NMR (101 MHz, $CDCl_3$) δ 168.97, 160.56, 159.40, 148.43, 140.04, 136.45, 132.35, 131.83, 128.02, 126.02, 123.51, 122.86, 121.22, 120.55, 113.89, 66.34, 64.81, 59.95, 53.78, 45.51, 42.80, 24.41; HRMS (ESI): $(M-H)^-$ ($C_{25}H_{31}ClN_6O_2$) cacld 481.2119, found 481.2107; elemental analysis calcd (%) for $C_{25}H_{31}ClN_6O_2$: C 62.17, H 6.47, N 17.40; Found: C 62.24, H 6.36, N 17.55.

*5.1.1.6. N-(5-Chloro-2-(4-(3-(dimethylamino)propylamino)quinazolin-2-yl)phenyl)-2-(2-(pyrrolidin-1-yl)ethylamino)acetamide (**10f**).* The compound **7** was treated with excess 2-(pyrrolidin-1-yl) ethanamine according to general aminolysis procedure to afford **10f**. After column chromatography with $CHCl_3/MeOH/NH_3\cdot H_2O$ (50:1:0.1) elution, the desired product was obtained as a white solid in 44% yield. mp 146–148 °C; ^{1}H NMR (400 MHz, $CDCl_3$): δ 14.04 (s, 1H), 8.94 (s, 1H), 8.90 (s, 1H), 8.60 (d, J = 8.6 Hz, 1H), 7.95 (d, J = 8.2 Hz, 1H), 7.68 (t, J = 7.6 Hz, 1H), 7.58 (d, J = 8.2 Hz, 1H), 7.41 (t, J = 7.6 Hz, 1H), 7.10 (d, J = 8.4 Hz, 1H), 3.84 (dd, J = 10.0, 5.2 Hz, 2H), 3.58 (s, 2H), 2.76 (t, J = 6.0 Hz, 2H), 2.63–2.57 (m, 2H), 2.51 (t, J = 6.0 Hz, 2H), 2.42 (t, J = 6.0 Hz, 4H), 2.37 (s, 6H), 2.11 (s, 1H), 1.96–1.88 (m, 2H), 1.80–1.67 (m, 4H); ^{13}C NMR (101 MHz, $CDCl_3$): δ 171.48, 160.57, 159.36, 148.62, 140.53, 136.60, 132.36, 131.85, 128.03, 125.83, 123.16, 122.67, 121.06, 120.49, 113.91, 59.93, 55.63, 54.79, 54.11, 48.42, 45.51, 42.71, 24.54, 23.49; HRMS (ESI): $(M-H)^-$ ($C_{27}H_{36}ClN_7O$) Cacld 508.2592, found 508.2585; elemental analysis calcd (%) for $C_{27}H_{36}ClN_7O\cdot H_2O$: C 61.41, H 7.25, N, 18.57; found: C 61.22, H 7.21, N 18.50.

*5.1.1.7. N-(5-Chloro-2-(4-(3-(dimethylamino)propylamino)quinazolin-2-yl)phenyl)-2-(2-(piperidin-1-yl)ethylamino)acetamide (**10g**).* The compound **7** was treated with excess 2-(piperidin-1-yl) ethanamine according to general aminolysis procedure to afford **10g**. After column chromatography with $CHCl_3/MeOH/NH_3\cdot H_2O$ (50:1:0.1) elution, the desired product was obtained as a white solid in 47% yield. mp 140-142 °C; ^{1}H NMR (400 MHz, $CDCl_3$): δ 14.04 (s, 1H), 8.95 (s, 1H), 8.91 (d, J = 2.0 Hz, 1H), 8.61 (d, J = 8.6 Hz, 1H), 7.96 (d, J = 8.4 Hz, 1H), 7.69 (t, J = 7.6 Hz, 1H), 7.59 (d, J = 8.0 Hz, 1H), 7.43 (t, J = 7.4 Hz, 1H), 7.11 (dd, J = 8.6, 1.9 Hz, 1H), 3.86 (dd, J = 10.0, 5.4 Hz, 2H), 3.59 (s, 2H), 2.75 (t, J = 6.2 Hz, 2H), 2.66–2.60 (m, 2H), 2.40 (s, 6H), 2.38–2.34 (m, 2H), 2.34–2.13 (m, 4H), 2.07 (s, 1H), 1.90 (dt, J = 10.8, 5.6 Hz, 2H), 1.55 (dt, J = 10.6, 5.2 Hz, 4H), 1.44–1.35 (m, 2H); ^{13}C NMR (101 MHz, $CDCl_3$): δ 171.55, 160.49, 159.30, 148.58, 140.48, 136.50, 132.25, 131.83, 127.97, 125.78, 123.17, 122.61, 121.04, 120.43, 113.87, 59.90, 58.24, 54.84, 54.59, 46.56, 45.50, 42.68, 26.01, 24.53, 24.46; HRMS (ESI): $(M-H)^-$ ($C_{28}H_{38}ClN_7O$) calcd 522.2748, found 522.2745. elemental analysis

calcd (%) for $C_{28}H_{38}ClN_7O{\cdot}H_2O$: C 62.03, H 7.44, N, 18.09; found: C 62.14, H 7.45, N 18.17.

*5.1.1.8. N-(5-Chloro-2-(4-(3-(dimethylamino)propylamino)quinazolin-2-yl)phenyl)-2-(3-(dimethylamino)propylamino)a-cetamide (**10h**).* The compound **7** was treated with excess N^1,N^1-dimethylpropane-1,3-diamine according to general aminolysis procedure to afford **10h**. After column chromatography with $CHCl_3$/MeOH/$NH_3{\cdot}H_2O$ (50:1:0.1) elution, the desired product was obtained as a white solid in 55% yield. mp 153–154 °C; ^{1}H NMR (400 MHz, $CDCl_3$): δ 14.05 (s, 1H), 8.99 (s, 1H), 8.89 (d, *J* = 2.2 Hz, 1H), 8.62 (d, *J* = 8.6 Hz, 1H), 7.88 (d, *J* = 8.2 Hz, 1H), 7.71 (t, *J* = 7.6 Hz, 1H), 7.60 (d, *J* = 8.0 Hz, 1H), 7.44 (t, *J* = 7.4 Hz, 1H), 7.12 (dd, *J* = 8.6, 2.2 Hz, 1H), 3.87 (dd, *J* = 10.2, 5.6 Hz, 2H), 3.60 (s, 2H), 2.74 (t, *J* = 7.2 Hz, 2H), 2.67–2.61 (m, 2H), 2.41 (s, 6H), 2.29 (t, *J* = 7.2 Hz, 2H), 2.15 (s, 6H), 1.96 (s, 1H), 1.93–1.90 (m, 2H), 1.70–1.62 (m, 2H); ^{13}C NMR (101 MHz, $CDCl_3$): δ 171.21, 160.47, 159.25, 148.37, 140.47, 136.55, 132.41, 131.83, 127.74, 125.87, 122.90, 122.66, 121.12, 120.34, 113.86, 59.89, 57.80, 54.62, 48.45, 45.51, 45.43, 42.72, 27.88, 24.44,; HRMS (ESI): $(M-H)^-$ ($C_{26}H_{36}ClN_7O$) cacld 496.2592, found 496.2588; elemental analysis calcd (%) for $C_{26}H_{36}ClN_7O{\cdot}H_2O$: C 60.51, H 7.42, N 19.00; found: C 60.47, H 7.45, N 19.03.

*5.1.1.9. N-(5-Chloro-2-(4-(3-(dimethylamino)propylamino)quinazolin-2-yl)phenyl)-2-(3-(diethylamino)propylamino)ac-etamide (**10i**).* The compound **7** was treated with excess N^1,N^1-diethylpropane-1,3-diamine according to general aminolysis procedure to afford **10i**. After column chromatography with $CHCl_3$/MeOH/$NH_3{\cdot}H_2O$ (50:1:0.1) elution, the desired product was obtained as a white solid in 57% yield. mp 149–151 °C; ^{1}H NMR (400 MHz, $CDCl_3$): δ 14.05 (s, 1H), 9.00 (s, 1H), 8.89 (d, *J* = 2.2 Hz, 1H), 8.62 (d, *J* = 8.6 Hz, 1H), 7.89 (d, *J* = 8.2 Hz, 1H), 7.75–7.68 (m, 1H), 7.61 (d, *J* = 8.2 Hz, 1H), 7.48–7.41 (m, 1H), 7.13 (dd, *J* = 8.6, 2.2 Hz, 1H), 3.87 (dd, *J* = 10.2, 5.6 Hz, 2H), 3.60 (s, 2H), 2.74 (t, *J* = 7.0 Hz, 2H), 2.68–2.62 (m, 2H), 2.51 (dd, *J* = 13.2, 6.8 Hz, 6H), 2.42 (d, *J* = 5.6 Hz, 6H), 2.08 (s, 1H), 1.91 (dd, *J* = 11.2, 5.6 Hz, 2H), 1.73–1.63 (m, 2H), 0.99 (t, *J* = 7.2 Hz, 6H); ^{13}C NMR ($CDCl_3$, 101 MHz): δ 171.33, 160.50, 159.28, 148.46, 140.48, 136.53, 132.34, 131.83, 127.82, 125.82, 123.01, 122.63, 121.06, 120.38, 113.87, 59.94, 54.64, 51.13, 48.84, 46.79, 45.51, 42.75, 27.13, 24.49, 11.68; HRMS (ESI): $(M-H)^-$ ($C_{28}H_{40}ClN_7O$) calcd 524.2905, found 524.2900; elemental analysis calcd (%) for $C_{28}H_{40}ClN_7O{\cdot}H_2O$: C 61.80, H 7.78, N 18.02; found: C 61.62, H 7.61, N 17.93.

*5.1.1.10. N-(5-Chloro-2-(4-(3-(dimethylamino)propylamino)-quinazolin-2-yl)phenyl)-3-(piperidin-1-yl)propanamide (**11a**).* The compound **8** was treated with excess piperidine according to general aminolysis procedure to afford **11a**. After column chromatography with $CHCl_3$/MeOH/$NH_3{\cdot}H_2O$ (50:1:0.1) elution, the desired product was obtained as a white solid in 69% yield. mp 178–179 °C; ^{1}H NMR (400 MHz, $CDCl_3$): δ 14.06 (s, 1H), 9.06 (s, 1H), 8.85 (d, *J* = 2.0 Hz, 1H), 8.66 (d, *J* = 8.6 Hz, 1H), 7.79–7.68 (m, 2H), 7.59 (d, *J* = 8.2 Hz, 1H), 7.48–7.40 (m, 1H), 7.08 (dd, *J* = 8.6, 2.2 Hz, 1H), 3.84 (dd, *J* = 10.2, 5.6 Hz, 2H), 2.92–2.82 (m, 2H), 2.80–2.71 (m, 2H), 2.67–2.58 (m, 2H), 2.54–2.42 (m, 4H), 2.40 (s, 6H), 1.96–1.85 (m, 2H), 1.61–1.53 (m, 4H), 1.46–1.37 (m, 2H); ^{13}C NMR (101 MHz, $CDCl_3$): δ 170.93, 160.60, 159.11, 148.02, 141.16, 136.75, 132.58, 131.74, 127.45, 125.93, 122.33, 121.79, 121.21, 120.01, 113.86, 59.94, 54.99, 54.42, 45.51, 42.83, 36.52, 25.97, 24.39, 24.30; HRMS (ESI): $(M-H)^-$ ($C_{27}H_{35}ClN_6O$) cacld 493.2483, found 493.2472; elemental analysis calcd (%) for $C_{27}H_{35}ClN_6O$: C 65.51, H 7.13, N 16.98; found: C 65.70, H 7.24, N 16.86.

*5.1.1.11. N-(5-Chloro-2-(4-(3-(dimethylamino)propylamino)-quinazolin-2-yl)phenyl)-3-(pyrrolidin-1-yl)propanamide (**11b**).* The compound **8** was treated with excess pyrrolidine according to general aminolysis procedure to afford **11b**. After column chromatography with $CHCl_3$/MeOH/$NH_3{\cdot}H_2O$ (50:1:0.1) elution, the desired product was obtained as a white solid in 71% yield. mp 163–165 °C; ^{1}H NMR (400 MHz, $CDCl_3$): δ 14.12 (s, 1H), 9.07 (s, 1H), 8.86 (d, *J* = 2.0 Hz, 1H), 8.67 (d, *J* = 8.6 Hz, 1H), 7.74 (dt, *J* = 15.0, 7.6 Hz, 2H), 7.60 (d, *J* = 8.2 Hz, 1H), 7.45 (dd, *J* = 11.0, 4.0 Hz, 1H), 7.10 (dd, *J* = 8.6, 2.2 Hz, 1H), 3.87 (dd, *J* = 10.2, 5.4 Hz, 2H), 3.01 (t, *J* = 7.6 Hz, 2H), 2.82 (t, *J* = 7.6 Hz, 2H), 2.74–2.55 (m, 6H), 2.41 (s, 6H), 1.97–1.88 (m, 2H), 1.86–1.74 (m, 4H); ^{13}C NMR (101 MHz, $CDCl_3$): δ 170.62, 160.68, 159.16, 148.07, 141.15, 136.84, 132.64, 131.73, 127.50, 125.94, 122.39, 121.81, 121.19, 120.09, 113.88, 59.96, 54.18, 52.08, 45.51, 42.84, 38.41, 24.40, 23.52; HRMS (ESI): Cacld for $(M-H)^-$ ($C_{26}H_{33}ClN_6O$) requires *m/z* 479.2326, found 479.2318; elemental analysis calcd (%) for $C_{26}H_{33}ClN_6O$: C 64.92, H 6.91, N 17.47; found: C 65.02, H 6.68, N 17.55.

*5.1.1.12. N-(5-Chloro-2-(4-(3-(dimethylamino)propylamino)-quinazolin-2-yl)phenyl)-3-(diethylamino)propanamide (**11c**).* The compound **8** was treated with excess diethylamine according to general aminolysis procedure to afford **11c**. After column chromatography with $CHCl_3$/MeOH/$NH_3{\cdot}H_2O$ (50:1:0.1) elution, the desired product was obtained as a white solid in 60% yield. mp 158–160 °C; ^{1}H NMR (400 MHz, $CDCl_3$): δ 14.08 (s, 1H), 9.07 (s, 1H), 8.86 (d, *J* = 2.1 Hz, 1H), 8.67 (d, *J* = 8.6 Hz, 1H), 7.77–7.68 (m, 2H), 7.59 (d, *J* = 8.1 Hz, 1H), 7.44 (ddd, *J* = 8.1, 6.1, 2.0 Hz, 1H), 7.09 (dd, *J* = 8.6, 2.2 Hz, 1H), 3.86 (dd, *J* = 10.2, 5.6 Hz, 2H), 3.07–2.95 (m, 2H), 2.76–2.68 (m, 2H), 2.64 (t, *J* = 4.2 Hz, 2H), 2.63–2.56 (m, 4H), 2.41 (s, 6H), 1.97–1.85 (m, 2H), 1.05 (t, *J* = 7.2 Hz, 6H); ^{13}C NMR (101 MHz, $CDCl_3$): δ 171.05, 160.60, 159.10, 147.99, 141.19, 136.74, 132.56, 131.74, 127.35, 125.93, 122.31, 121.74, 121.24, 119.95, 113.87, 59.90, 48.93, 47.01, 45.49, 42.73, 36.64, 24.41, 11.90. HRMS (ESI): $(M-H)^-$ ($C_{26}H_{35}ClN_6O$) cacld 481.2483, found 481.2472; elemental analysis calcd (%) for $C_{26}H_{35}ClN_6O{\cdot}H_2O$: C 62.32, H 7.44, N 16.77; found: C 62.15, H 7.57, N 16.63.

*5.1.1.13. N-(5-Chloro-2-(4-(3-(dimethylamino)propylamino)-quinazolin-2-yl)phenyl)-3-(4-methylpiperazin-1-yl)propane-mide (**11d**).* The compound **8** was treated with excess *N*-methyl piperazine according to general aminolysis procedure to afford **11d**. After column chromatography with $CHCl_3$/MeOH/$NH_3{\cdot}H_2O$ (50:1:0.1) elution, the desired product was obtained as a white solid in 44% yield. mp 167–168 °C; ^{1}H NMR (400 MHz, $CDCl_3$): δ 14.07 (s, 1H), 9.07 (s, 1H), 8.85 (d, *J* = 1.6 Hz, 1H), 8.66 (d, *J* = 8.6 Hz, 1H), 7.72 (d, *J* = 4.0 Hz, 2H), 7.60 (d, *J* = 8.2 Hz, 1H), 7.45 (dt, *J* = 8.2, 4.0 Hz, 1H), 7.09 (dd, *J* = 8.6, 1.8 Hz, 1H), 3.86 (dd, *J* = 10.2, 5.4 Hz, 2H), 2.92 (t, *J* = 7.4 Hz, 2H), 2.75 (t, *J* = 7.4 Hz, 2H), 2.67–2.63 (m, 2H), 2.59 (dd, *J* = 19.2, 11.0 Hz, 4H), 2.49–2.41 (m, 4H), 2.41 (s, 6H), 2.26 (s, 3H), 1.95–1.87 (m, 2H); ^{13}C NMR (101 MHz, $CDCl_3$): δ 170.62, 160.71, 159.19, 148.08, 141.12, 136.87, 132.69, 131.77, 127.40, 125.98, 122.46, 121.85, 121.28, 120.12, 113.92, 59.92, 55.08, 54.20, 52.99, 46.01, 45.51, 42.80, 36.39, 24.42; HRMS (ESI): $(M-H)^-$ ($C_{27}H_{36}ClN_7O$) cacld 508.2592, found 508.2588; elemental analysis calcd (%) for $C_{27}H_{36}ClN_7O$: C 63.58, H 7.11, N 19.22; found: C 63.49, H 7.26, N 19.36.

*5.1.1.14. N-(5-Chloro-2-(4-(3-(dimethylamino)propylamino)quinazolin-2-yl)phenyl)-3-morpholinopropanamide (**11e**).* The compound **8** was treated with excess morpholine according to general aminolysis procedure to afford **11e**. After column chromatography with $CHCl_3$/MeOH/$NH_3{\cdot}H_2O$ (50:1:0.1) elution, the desired product was obtained as a white solid in 67% yield. mp 165–167 °C; ^{1}H NMR (400 MHz, $CDCl_3$): δ 14.10 (s, 1H), 9.08 (s, 1H), 8.84 (d, *J* = 2.0 Hz, 1H), 8.67 (d, *J* = 8.6 Hz, 1H), 7.75–7.69 (m, 2H), 7.62 (d, *J* = 8.2 Hz, 1H), 7.45 (ddd, *J* = 8.2, 5.2, 3.0 Hz, 1H), 7.10 (dd, *J* = 8.6, 2.2 Hz, 1H),

3.86 (dd, J = 10.2, 5.4 Hz, 2H), 3.69–3.61 (m, 4H), 2.89 (t, J = 7.2 Hz, 2H), 2.75 (t, J = 7.2 Hz, 2H), 2.68–2.62 (m, 2H), 2.58–2.48 (m, 4H), 2.42 (s, 6H), 1.95–1.89 (m, 2H); ^{13}C NMR (101 MHz, $CDCl_3$): δ 170.52, 160.59, 159.12, 147.94, 141.04, 136.77, 132.63, 131.77, 127.20, 125.99, 122.46, 121.80, 121.34, 120.02, 113.88, 66.88, 59.72, 54.61, 53.53, 45.46, 42.61, 36.28, 24.44; HRMS (ESI): $(M - H)^-$ ($C_{26}H_{33}ClN_6O_2$) cacld 495.2275, found 495.2271; elemental analysis calcd (%) for $C_{26}H_{33}Cl\ N_6O_2H_2O$: C 60.63, H 6.85, N 16.32; found: C 60.51, H 6.92, N 16.36.

*5.1.1.15. N-(5-Chloro-2-(4-(3-(dimethylamino)propylamino)-quinazolin-2-yl)phenyl)-4-(piperidin-1-yl)butanamide (**12a**).* The compound **9** was treated with excess piperidine according to general aminolysis procedure to afford **12a**. After column chromatography with $CHCl_3$/MeOH/$NH_3\cdot H_2O$ (50:1:0.1) elution, the desired product was obtained as a white solid in 73% yield. mp 159–160 °C; ^{1}H NMR (400 MHz, $CDCl_3$): δ 14.04 (s, 1H), 9.03 (s, 1H), 8.86 (d, J = 2.2 Hz, 1H), 8.68 (d, J = 8.6 Hz, 1H), 7.80–7.70 (m, 2H), 7.61 (d, J = 8.0 Hz, 1H), 7.45 (ddd, J = 8.2, 6.2, 2.0 Hz, 1H), 7.10 (dd, J = 8.6, 2.2 Hz, 1H), 3.87 (dd, J = 10.2, 5.6 Hz, 2H), 2.69–2.62 (m, 2H), 2.59 (t, J = 7.4 Hz, 2H), 2.53–2.46 (m, 2H), 2.46–2.41 (m, 4H), 2.41 (s, 6H), 2.04 (dt, J = 14.8, 7.4 Hz, 2H), 1.92 (dt, J = 11.2, 5.8 Hz, 2H), 1.56 (dt, J = 11.0, 5.4 Hz, 4H), 1.45–1.36 (m, 2H); ^{13}C NMR (101 MHz, $CDCl_3$): δ 171.94, 160.74, 159.20, 148.17, 141.29, 136.90, 132.64, 131.77, 127.54, 125.94, 122.33, 121.81, 121.23, 120.05, 113.92, 60.00, 58.70, 54.56, 45.53, 42.86, 36.90, 25.95, 24.45, 23.42, 22.94; HRMS (ESI): $(M - H)^-$ ($C_{28}H_{37}ClN_6O$) calcd 507.2639, found 507.2629; elemental analysis calcd (%) for $C_{28}H_{37}ClN_6O$: C 66.06, H 7.33, N 16.51; found: C 66.10, H 7.49, N 16.32.

*5.1.1.16. N-(5-Chloro-2-(4-(3-(dimethylamino)propylamino)quinazolin-2-yl)phenyl)-4-(4-methylpiperazin-1-yl)butanami-de (**12d**).* The compound **9** was treated with excess *N*-methyl piperazine according to general aminolysis procedure to afford **12d**. After column chromatography with $CHCl_3$/MeOH/$NH_3\cdot H_2O$ (50:1:0.1) elution, the desired product was obtained as a white solid in 58% yield. mp 155–157 °C; ^{1}H NMR (400 MHz, $CDCl_3$): δ 14.03 (s, 1H), 9.02 (s, 1H), 8.85 (d, J = 2.2 Hz, 1H), 8.66 (d, J = 8.6 Hz, 1H), 7.72 (dd, J = 4.0, 1.6 Hz, 2H), 7.60 (d, J = 8.2 Hz, 1H), 7.43 (ddd, J = 8.2, 5.4, 2.8 Hz, 1H), 7.08 (dd, J = 8.6, 2.2 Hz, 1H), 3.89 (dd, J = 10.2, 5.6 Hz, 2H), 2.75–2.69 (m, 2H), 2.66 (t, J = 7.4 Hz, 2H), 2.59 (t, J = 7.4 Hz, 2H), 2.55–2.46 (m, 4H), 2.43 (s, 6H), 2.36–2.28 (m, 4H), 2.23 (s, 3H), 2.02 (dt, J = 14.6, 7.4 Hz, 2H), 1.97–1.90 (m, 2H); ^{13}C NMR (101 MHz, $CDCl_3$): δ 171.86, 160.64, 159.12, 148.05, 141.26, 136.80, 132.60, 131.75, 127.42, 125.91, 122.26, 121.71, 121.26, 119.95, 113.89, 59.89, 57.81, 55.10, 53.11, 45.99, 45.49, 42.76, 36.75, 24.41, 22.93; HRMS (ESI): $(M - H)^-$ ($C_{28}H_{38}ClN_7O$) cacld 522.2748, found 522.2747; elemental analysis calcd (%) for $C_{28}H_{38}ClN_7O$: C 64.17, H 7.31, N 18.71; found: C 64.03, H 7.26, N 18.59.

*5.1.1.17. N-(5-Chloro-2-(4-(3-(dimethylamino)propylamino)quinazolin-2-yl)phenyl)-4-morpholinobutanamide (**12e**).* The compound **9** was treated with excess morpholine according to general aminolysis procedure to afford **12e**. After column chromatography with $CHCl_3$/MeOH/$NH_3\cdot H_2O$ (50:1:0.1) elution, the desired product was obtained as a white solid in 65% yield. mp 152–154 °C; ^{1}H NMR (400 MHz, $CDCl_3$): δ 14.07 (s, 1H), 9.03 (s, 1H), 8.87 (d, J = 2.2 Hz, 1H), 8.68 (d, J = 8.6 Hz, 1H), 7.78–7.69 (m, 2H), 7.65 (d, J = 8.2 Hz, 1H), 7.46 (ddd, J = 8.2, 5.0, 3.2 Hz, 1H), 7.10 (dd, J = 8.6, 2.2 Hz, 1H), 3.88 (dd, J = 10.4, 5.6 Hz, 2H), 3.70–3.56 (m, 4H), 2.73–2.64 (m, 2H), 2.61 (t, J = 7.2 Hz, 2H), 2.47 (t, J = 6.4 Hz, 2H), 2.44 (s, 6H), 2.08–1.99 (m, 2H), 1.98–1.91 (m, 2H), 1.86–1.72 (m, 4H); ^{13}C NMR (101 MHz, $CDCl_3$): δ 171.82, 160.65, 159.12, 148.02, 141.24, 136.83, 132.60, 131.77, 127.30, 125.96, 122.32, 121.68, 121.32, 119.93, 113.89, 66.97, 59.81, 58.27, 53.67, 45.48, 42.68, 36.62, 24.43, 22.52; HRMS (ESI): $(M - H)^-$ ($C_{27}H_{35}ClN_6O_2$) cacld 509.2432, found 509.2429; elemental analysis calcd (%) for $C_{27}H_{35}ClN_6O_2$: C 63.45, H 6.90, N 16.44; found: C 63.31, H 7.05, N 16.51.

5.2. Materials

All oligomers/primers used in this study were purchased from Invitrogen (China). Stock solutions of all the derivatives (10 mM) were made using DMSO (10%) or double-distilled deionized water. Further dilutions to working concentrations were made with double-distilled deionized water.

5.3. FRET assay

FRET assay was carried out on a real-time PCR apparatus following previously published procedures [52]. The fluorescently labeled oligonucleotides F21T: 5′-FAM-d(GGG[TTAGGG]$_3$)-TAMRA-3′ and F10T: 5′-FAM-dTATAGCTATA-HEG-TATAGCTATA-TAMRA-3′ (donor fluorophore FAM is 6-carboxyfluorescein; acceptor fluorophore TAMRA is 6-carboxytetramethylrhodamine; HEG linker is [(CH_2–CH_2–O)$_6$]) were used as the FRET probes. Fluorescence melting curves were determined with a Roche LightCycler 2 real-time PCR machine, using a total reaction volume of 20 μL, with 0.2 μM of labeled oligonucleotide in Tris–HCl buffer (10 mM, pH 7.4) containing 60 mM KCl. Fluorescence readings with excitation at 470 nm and detection at 530 nm were taken at intervals of 1 °C over the range 37–99 °C, with a constant temperature being maintained for 30 s prior to each reading to ensure a stable value. The melting of the G-quadruplex was monitored alone or in the presence of various concentrations of compounds and/or of double-stranded competitor ds26. Final analysis of the data was carried out using Origin7.5 (OriginLab Corp.).

5.4. Surface plasmon resonance

SPR measurements were performed on a ProteOn XPR36 Protein Interaction Array system (Bio-Rad Laboratories, Hercules, CA) using a Neutravidin-coated GLH sensor chip. In a typical experiment, biotinylated duplex DNA and biotinylated HTG21 (5′-d(GGG[TTAGGG]$_3$)-3′) were folded in filtered and degassed running buffer (Tris–HCl 50 mM pH 7.2, 100 mM KCl). The DNA samples were then captured (~1000 RU) in flow cells 1 and 2, leaving the third flow cell as a blank. Ligand solutions (at 0.15625, 0.3125, 0.625, 1.25, 2.5, 5, 10, and 20 μM) were prepared with running buffer by serial dilutions from stock solutions. Six concentrations were injected simultaneously at a flow rate of 100 mL min^{-1} for 150 s of association phase, followed with 300 s of dissociation phase at 25 °C. The NLC sensor chip was regenerated with short injection of 1 M NaCl between consecutive measurements. The final graphs were obtained by subtracting blank sensorgrams from the duplex or quadruplex sensorgrams. Data are analyzed with ProteOn manager software, using the Langmuir model for fitting kinetic data.

5.5. CD measurements

The oligomer HTG21 (5′-d(GGG[TTAGGG]$_3$)-3′) at a final concentration of 5 μM was resuspended in Tris–HCl buffer (10 mM, pH 7.2) containing the derivatives to be tested. The samples were heated to 95 °C, then gradually cooled to room temperature, and incubated at 4 °C for at least 6 h. The CD spectra were recorded on Chirascan (AppliedPhotophysics) spectrophotometer. A quartz cuvette with 4 mm path length was used for the spectra recorded over a wavelength range of 230–450 at 1 nm bandwidth, 1 nm step size, and 0.5 s time per point. The CD spectra were obtained by taking the average of two scans made from 230 to 450 nm. Final

analysis of the data was carried out using Origin 7.5 (OriginLab Corp.).

5.6. NMR spectroscopy

NMR experiments were performed on a Bruker AVANCE AV 400 MHz spectrometer. The ^{1}H NMR spectrum of **11d** was obtained in a 90% H_2O/10% D_2O solution containing 150 mM KCl and 25 mM potassium phosphate buffer with varying pH values of 3.0, 3.5, 4.0, 5.0, 6.0, and 7.0 respectively. All of the titration experiments were carried out at 25 °C in a 90% H_2O/10% D_2O solution containing 150 mM KCl and 25 mM potassium phosphate buffer (pH = 7.0). Water suppression was achieved by the Watergate method. The oligonucleotide d(TTAGGG) was purified by using HPLC, and the concentration was 0.5 mM for the NMR measurements.

5.7. Molecular modelling

The crystal structure of the mixed hybrid-type 26-mer telomeric G-quadruplex (PDB ID 2HY9) [61,62] was used as an initial model to study the interaction between the quindoline derivatives and telomeric DNA. The terminal 5′ adenine residue was removed to generate a 21-mer structure, for comparison with the d(GGG[TTAGGG]$_3$) DNA we used in the FRET and CD experiments. Water molecules were removed from the PDB file, and the missing hydrogen atoms were added to the system using the Biopolymer module implemented in the SYBYL7.3.5 molecular modeling software from Tripos Inc. (St. Louis, MO). Ligand structures were constructed by adopting the empirical Gasteiger Huckel (GH) partial atomic charges and then were optimized (Tripos force field) with a nonbond cutoff of 12 Å and a convergence of 0.01 kcal mol^{-1}/Å over 10,000 steps using the Powell conjugate-gradient algorithm.

Docking studies were carried out using the AUTODOCK 4.0 program [69]. By using ADT [70], nonpolar hydrogens of telomeric G-quadruplex were merged to their corresponding carbons, and partial atomic charges were assigned. The nonpolar hydrogens of the ligands were merged, and rotatable bonds were assigned. The resulting G-quadruplex structure was used as an input for the AUTOGRID program. AUTOGRID gave a precalculated atomic affinity grid maps for each atom type in the ligand, plus an electrostatics map and a separate desolvation map present in the substrate molecule. The dimensions of the active site box, which was placed at the center of the G-quadruplex, were set to 54 Å × 54 Å × 54 Å with the grid points 0.375 Å apart. Docking calculations were carried out using the Lamarckian genetic algorithm (LGA). Initially, we used a population of random individuals (population size: 150), a maximum number of 25,000,000 energy evaluations, a maximum number of generations of 27,000, and a mutation rate of 0.02. One hundred independent docking runs were carried out for each ligand. The resulting positions were clustered according to a root-mean-square criterion of 0.5 Å.

5.8. TRAP-LIG assay

The ability of quinazoline derivatives to inhibit telomerase in a cell-free system was assessed with the TRAP-LIG assay following previously published procedures [63]. Protein extracts from exponentially growing MCF-7 breast carcinoma cells were used. Briefly, 0.1 μg of TS forward primer (5′-AATCCGTC-GAGCAGAGTT-3′) was elongated by telomerase (500 ng protein extract) in TRAP buffer (20 mM Tris–HCl [pH 8.3], 68 mM KCl, 1.5 mM $MgCl_2$, 1 mM EGTA, and 0.05% Tween 20) containing 125 μM dNTPs and 0.05 μg BSA. The mix was added to tubes containing freshly prepared ligand at various concentrations and to a negative control containing no ligand. The initial elongation step was carried out for 20 min at 30 °C, followed by 94 °C for 5 min and a final maintenance of the mixture at 20 °C. To purify the elongated product and to remove the bound ligands, the QIA quick nucleotide purification kit (Qiagen) was used according to the manufacturer's instructions. The purified extended samples were then subject to PCR amplification. For this, a second PCR master mix was prepared consisting of 1 μM ACX reverse primer (5′-GCGCGG[CTTACC]$_3$CTAACC-3′), 0.1 μg TS forward primer (5′-AATCCGTCGAGCAGAGTT-3′), TRAP buffer, 5 μg BSA, 0.5 mM dNTPs, and 2 units of Taq polymerase. A 10 μL aliquot of the master mix was added to the purified telomerase extended samples and amplified for 35 cycles of 94 °C for 30 s, of 61 °C for 1 min, and of 72 °C for 1 min. Samples were separated on a 16% PAGE and visualized with silver-stained. Tel IC_{50} values were then calculated from the optical density quantitated from the AlphaEaseFC software.

5.9. Short-term cell viability

HL60 leukemia cell line was seeded on 96-well plates (1.0×10^3 well^{-1}) and exposed to various concentrations of derivatives. After 48 h of treatment at 37 °C in a humidified atmosphere of 5% CO_2, 10 μL of 5 mg/mL^{-1} methyl thiazolyl tetrazolium (MTT) solution was added to each well and further incubated for 4 h. The cells in each well were then treated with dimethyl sulfoxide (DMSO) (200 μL for each well), and the optical density (OD) was recorded at 570 nm. All drug doses were parallel tested in triplicate, and the IC_{50} values were derived from the mean OD values of the triplicate tests versus drug concentration curves.

5.10. Long-term cell culture experiments

Long-term proliferation experiments were carried out using the HL60 leukemia cell line. Cells (1.0×10^5) were grown in 10 cm Petri dishes and exposed to a subcytotoxic concentration of a ligand or an equivalent volume of 0.1% DMSO every 4 days. The cells in control and drug-exposed flasks were counted and flasks reseeded with 1.0×10^5 cells. The remaining cells were collected and used for the measurements described below. This process was continued for 16 days.

5.11. SA-β-Gal assay

After the long-term incubation, the growth medium was aspirated and the cells were fixed in 2% formaldehyde/0.2% glutaraldehyde for 15 min at room temperature. The fixing solution was removed, and the cells were gently washed twice with PBS and then stained using the β-Gal stain solution containing 1 mg/mL of 5-bromo-4-chloro-3-indolyl-β-D-galactoside, followed by incubation overnight at 37 °C. The staining solution was removed, and the cells were washed three times with PBS. The cells were viewed under an optical microscope and photographed.

5.12. Telomere length assay

Cells were incubated with the ligand for 16 days. To measure the telomere length, genomic DNA was digested with Hinf1/Rsa1 restriction enzymes. The digested DNA fragments were separated on 0.8% agarose gel, transferred to a nylon membrane, and the transferred DNA fixed on the wet blotting membrane by baking the membrane at 120 °C for 20 min. The membrane was hybridized with a DIG-labeled hybridization probe for telomeric repeats and incubated with anti-DIG-alkaline phosphatase. TRF was performed with chemiluminescence detection.

Acknowledgements

We thank the Natural Science Foundation of China (Grants U0832005, 90813011), the International S&T Cooperation Program of China (2010DFA34630), the Specialized Research Fund for the Doctoral Program of Higher Education (20090171110050), and the Science Foundation of Guangzhou (2009A1-E011-6) for financial support of this study.

Appendix. Supplementary data

Supplementary data associated with this article can be found, in the online version, at doi:10.1016/j.ejmech.2011.10.057.

References

[1] J.T. Davis, G-quartets 40 years later: from 5′-GMP to molecular biology and supramolecular chemistry, Angew. Chem. Int. Ed. Engl. 43 (2004) 668–698.
[2] S. Burge, G.N. Parkinson, P. Hazel, A.K. Todd, S. Neidle, Quadruplex DNA: sequence, topology and structure, Nucleic Acids Res. 34 (2006) 5402–5415.
[3] J.L. Huppert, Four-stranded nucleic acids: structure, function and targeting of G-quadruplexes, Chem. Soc. Rev. 37 (2008) 1375–1384.
[4] D. Monchaud, M.P. Teulade-Fichou, A hitchhiker's guide to G-quadruplex ligands, Org. Biomol. Chem. 6 (2008) 627–636.
[5] E. Henderson, C.C. Hardin, S.K. Walk, I. Tinoco Jr., E.H. Blackburn, Telomeric DNA oligonucleotides form novel intramolecular structures containing guanine-guanine base pairs, Cell 51 (1987) 899–908.
[6] M.A. Keniry, Quadruplex structures in nucleic acids, Biopolymers 56 (2000) 123–146.
[7] M.C. Hammond-Kosack, B. Dobrinski, R. Lurz, K. Docherty, M.W. Kilpatrick, The human insulin gene linked polymorphic region exhibits an altered DNA structure, Nucleic Acids Res. 20 (1992) 231–236.
[8] A. Yafe, S. Etzioni, P. Weisman-Shomer, M. Fry, Formation and properties of hairpin and tetraplex structures of guanine-rich regulatory sequences of muscle-specific genes, Nucleic Acids Res. 33 (2005) 2887–2900.
[9] A. Siddiqui-Jain, C.L. Grand, D.J. Bearss, L.H. Hurley, Direct evidence for a G-quadruplex in a promoter region and its targeting with a small molecule to repress c-MYC transcription, Proc. Natl. Acad. Sci. U S A 99 (2002) 11593–11598.
[10] D. Sun, K. Guo, J.J. Rusche, L.H. Hurley, Facilitation of a structural transition in the polypurine/polypyrimidine tract within the proximal promoter region of the human VEGF gene by the presence of potassium and G-quadruplex-interactive agents, Nucleic Acids Res. 33 (2005) 6070–6080.
[11] T.S. Dexheimer, D. Sun, L.H. Hurley, Deconvoluting the structural and drug-recognition complexity of the G-quadruplex-forming region upstream of the bcl-2 P1 promoter, J. Am. Chem. Soc. 128 (2006) 5404–5415.
[12] H. Fernando, A.P. Reszka, J. Huppert, S. Ladame, S. Rankin, A.R. Venkitaraman, S. Neidle, S. Balasubramanian, A conserved quadruplex motif located in a transcription activation site of the human c-kit oncogene, Biochemistry 45 (2006) 7854–7860.
[13] K. Nemoto, T. Kubo, M. Nomachi, T. Sano, T. Matsumoto, K. Hosoya, T. Hattori, K. Kaya, Simple and effective 3D recognition of Domoic acid using a Molecularly Imprinted Polymer, J. Am. Chem. Soc. 129 (2007) 13626–13632 J. Am. Chem. Soc., 130 (2008) 774.
[14] R. Rodriguez, S. Muller, J.A. Yeoman, C. Trentesaux, J.F. Riou, S. Balasubramanian, A novel small molecule that alters shelterin integrity and triggers a DNA-damage response at telomeres, J. Am. Chem. Soc. 130 (2008) 15758–15759.
[15] S. Neidle, G. Parkinson, Telomere maintenance as a target for anticancer drug discovery, Nat. Rev. Drug Discov. 1 (2002) 383–393.
[16] T.A. Brooks, L.H. Hurley, The role of supercoiling in transcriptional control of MYC and its importance in molecular therapeutics, Nat. Rev. Cancer 9 (2009) 849–861.
[17] V. Gonzalez, L.H. Hurley, The c-MYC NHE III(1): function and regulation, Annu. Rev. Pharmacol. Toxicol. 50 (2010) 111–129.
[18] V. Gonzalez, L.H. Hurley, The C-terminus of nucleolin promotes the formation of the c-MYC G-quadruplex and inhibits c-MYC promoter activity, Biochemistry 49 (2010) 9706–9714.
[19] V. Caprio, B. Guyen, Y. Opoku-Boahen, J. Mann, S.M. Gowan, L.M. Kelland, M.A. Read, S. Neidle, A novel inhibitor of human telomerase derived from 10H-indolo[3,2-b]quinoline, Bioorg. Med. Chem. Lett. 10 (2000) 2063–2066.
[20] K. Shin-ya, K. Wierzba, K. Matsuo, T. Ohtani, Y. Yamada, K. Furihata, Y. Hayakawa, H. Seto, Telomestatin, a novel telomerase inhibitor from Streptomyces anulatus, J. Am. Chem. Soc. 123 (2001) 1262–1263.
[21] B. Guyen, C.M. Schultes, P. Hazel, J. Mann, S. Neidle, Synthesis and evaluation of analogues of 10H-indolo[3,2-b]quinoline as G-quadruplex stabilising ligands and potential inhibitors of the enzyme telomerase, Org. Biomol. Chem. 2 (2004) 981–988.
[22] A. Biroccio, A. Rizzo, R. Elli, C.E. Koering, A. Belleville, B. Benassi, C. Leonetti, M.F. Stevens, M. D'Incalci, G. Zupi, E. Gilson, TRF2 inhibition triggers apoptosis and reduces tumourigenicity of human melanoma cells, Eur. J. Cancer 42 (2006) 1881–1888.
[23] M.J. Moore, C.M. Schultes, J. Cuesta, F. Cuenca, M. Gunaratnam, F.A. Tanious, W.D. Wilson, S. Neidle, Trisubstituted acridines as G-quadruplex telomere targeting agents. Effects of extensions of the 3,6- and 9-side chains on quadruplex binding, telomerase activity, and cell proliferation, J. Med. Chem. 49 (2006) 582–599.
[24] C. Leonetti, M. Scarsella, G. Riggio, A. Rizzo, E. Salvati, M. D'Incalci, L. Staszewsky, R. Frapolli, M.F. Stevens, A. Stoppacciaro, M. Mottolese, B. Antoniani, E. Gilson, G. Zupi, A. Biroccio, G-quadruplex ligand RHPS4 potentiates the antitumor activity of camptothecins in preclinical models of solid tumors, Clin. Cancer Res. 14 (2008) 7284–7291.
[25] Y.J. Lu, T.M. Ou, J.H. Tan, J.Q. Hou, W.Y. Shao, D. Peng, N. Sun, X.D. Wang, W.B. Wu, X.Z. Bu, Z.S. Huang, D.L. Ma, K.Y. Wong, L.Q. Gu, 5-N-methylated quindoline derivatives as telomeric g-quadruplex stabilizing ligands: effects of 5-N positive charge on quadruplex binding affinity and cell proliferation, J. Med. Chem. 51 (2008) 6381–6392.
[26] G. Zagotto, C. Sissi, L. Lucatello, C. Pivetta, S.A. Cadamuro, K.R. Fox, S. Neidle, M. Palumbo, Aminoacyl-anthraquinone conjugates as telomerase inhibitors: synthesis, biophysical and biological evaluation, J. Med. Chem. 51 (2008) 5566–5574.
[27] D. Gomez, N. Aouali, A. Renaud, C. Douarre, K. Shin-Ya, J. Tazi, S. Martinez, C. Trentesaux, H. Morjani, J.F. Riou, Resistance to senescence induction and telomere shortening by a G-quadruplex ligand inhibitor of telomerase, Cancer Res. 63 (2003) 6149–6153.
[28] A.D. Moorhouse, A.M. Santos, M. Gunaratnam, M. Moore, S. Neidle, J.E. Moses, Stabilization of G-quadruplex DNA by highly selective ligands via click chemistry, J. Am. Chem. Soc. 128 (2006) 15972–15973.
[29] J. Dash, P.S. Shirude, S.T. Hsu, S. Balasubramanian, Diarylethynyl amides that recognize the parallel conformation of genomic promoter DNA G-quadruplexes, J. Am. Chem. Soc. 130 (2008) 15950–15956.
[30] W.C. Drewe, R. Nanjunda, M. Gunaratnam, M. Beltran, G.N. Parkinson, A.P. Reszka, W.D. Wilson, S. Neidle, Rational design of substituted diarylureas: a scaffold for binding to G-quadruplex motifs, J. Med. Chem. 51 (2008) 7751–7767.
[31] S. Muller, G.D. Pantos, R. Rodriguez, S. Balasubramanian, Controlled-folding of a small molecule modulates DNA G-quadruplex recognition, Chem. Commun. (Camb) (2009) 80–82.
[32] J.E. Moses, D.J. Ritson, F. Zhang, C.M. Lombardo, S. Haider, N. Oldham, S. Neidle, A click chemistry approach to C3 symmetric, G-quadruplex stabilising ligands, Org. Biomol. Chem. 8 (2010) 2926–2930.
[33] J.H. Tan, T.M. Ou, J.Q. Hou, Y.J. Lu, S.L. Huang, H.B. Luo, J.Y. Wu, Z.S. Huang, K.Y. Wong, L.Q. Gu, Isaindigotone derivatives: a new class of highly selective ligands for telomeric G-quadruplex DNA, J. Med. Chem. 52 (2009) 2825–2835.
[34] J.F. Galan, J. Brown, J.L. Wildin, Z. Liu, D. Liu, G. Moyna, V. Pophristic, Intramolecular hydrogen bonding in ortho-substituted arylamide oligomers: a computational and experimental study of ortho-fluoro- and ortho-chloro-N-methylbenzamides, J. Phys. Chem. B. 113 (2009) 12809–12815.
[35] B. Kuhn, P. Mohr, M. Stahl, Intramolecular hydrogen bonding in medicinal chemistry, J. Med. Chem. 53 (2010) 2601–2611.
[36] R.B. Teklebrhan, K. Zhang, G. Schreckenbach, F. Schweizer, S.D. Wetmore, Intramolecular hydrogen bond-controlled prolyl amide isomerization in glucosyl 3(S)-hydroxy-5-hydroxymethylproline hybrids: a computational study, J. Phys. Chem. B. 114 (2010) 11594–11602.
[37] W.G. Harter, H. Albrect, K. Brady, B. Caprathe, J. Dunbar, J. Gilmore, S. Hays, C.R. Kostlan, B. Lunney, N. Walker, The design and synthesis of sulfonamides as caspase-1 inhibitors, Bioorg. Med. Chem. Lett. 14 (2004) 809–812.
[38] M.C. Van Zandt, E.O. Sibley, E.E. McCann, K.J. Combs, B. Flam, D.R. Sawicki, A. Sabetta, A. Carrington, J. Sredy, E. Howard, A. Mitschler, A.D. Podjarny, Design and synthesis of highly potent and selective (2-arylcarbamoyl-phenoxy)-acetic acid inhibitors of aldose reductase for treatment of chronic diabetic complications, Bioorg. Med. Chem. 12 (2004) 5661–5675.
[39] C.N. Hodge, J. Pierce, A diazine heterocycle replaces a six-membered hydrogen-bonded array in the active site of scytalone dehydratase, Bioorg. Med. Chem. Lett. 3 (1993) 1605–1608.
[40] P. Furet, G. Bold, F. Hofmann, P. Manley, T. Meyer, K.H. Altmann, Identification of a new chemical class of potent angiogenesis inhibitors based on conformational considerations and database searching, Bioorg. Med. Chem. Lett. 13 (2003) 2967–2971.
[41] P. Furet, G. Caravatti, V. Guagnano, M. Lang, T. Meyer, J. Schoepfer, Entry into a new class of protein kinase inhibitors by pseudo ring design, Bioorg. Med. Chem. Lett. 18 (2008) 897–900.
[42] K.A. Menear, C. Adcock, F.C. Alonso, K. Blackburn, L. Copsey, J. Drzewiecki, A. Fundo, A. Le Gall, S. Gomez, H. Javaid, C.F. Lence, N.M. Martin, C. Mydlowski, G.C. Smith, Novel alkoxybenzamide inhibitors of poly(ADP-ribose) polymerase, Bioorg. Med. Chem. Lett. 18 (2008) 3942–3945.
[43] J.Q. Hou, J.H. Tan, X.X. Wang, S.B. Chen, S.Y. Huang, J.W. Yan, S.H. Chen, T.M. Ou, H.B. Luo, D. Li, L.Q. Gu, Z.S. Huang, Impact of planarity of unfused aromatic molecules on G-quadruplex binding: learning from isaindigotone derivatives, Org. Biomol. Chem. 9 (2011) 6422–6436.
[44] R.J. Harrison, J. Cuesta, G. Chessari, M.A. Read, S.K. Basra, A.P. Reszka, J. Morrell, S.M. Gowan, C.M. Incles, F.A. Tanious, W.D. Wilson, L.R. Kelland, S. Neidle, Trisubstituted acridine derivatives as potent and selective telomerase inhibitors, J. Med. Chem. 46 (2003) 4463–4476.

[45] F. Gellibert, M.H. Fouchet, V.L. Nguyen, R. Wang, G. Krysa, A.C. de Gouville, S. Huet, N. Dodic, Design of novel quinazoline derivatives and related analogues as potent and selective ALK5 inhibitors, Bioorg. Med. Chem. Lett. 19 (2009) 2277–2281.
[46] A.D. Roy, A. Subramanian, R. Roy, Auto-redox reaction: tin(II) chloride-mediated one-step reductive cyclization leading to the synthesis of novel biheterocyclic 5,6-dihydro-quinazolino[4,3-b]quinazolin-8-ones with three-point diversity, J. Org. Chem. 71 (2006) 382–385.
[47] D.J. Connolly, P.M. Lacey, M. McCarthy, C.P. Saunders, A.M. Carroll, R. Goddard, P.J. Guiry, Preparation and resolution of a modular class of axially chiral quinazoline-containing ligands and their application in asymmetric rhodium-catalyzed olefin hydroboration, J. Org. Chem. 69 (2004) 6572–6589.
[48] R.A.W. Johnstone, A.H. Wilby, I.D. Entwistle, Heterogeneous catalytic transfer hydrogenation and its relation to other methods for reduction of organic compounds, Chem. Rev. 85 (1985) 129–170.
[49] B.W. Gung, Z. Zhu, D. Zou, B. Everingham, A. Oyeamalu, R.M. Crist, J. Baudlier, Requirement for hydrogen-bonding Cooperativity in small Polyamides: a Combined VT-NMR and VT-IR Investigation, J. Org. Chem. 63 (1998) 5750–5761.
[50] M. Avalos, R. Babiano, J.L. Barneto, J.L. Bravo, P. Cintas, J.L. Jimenez, J.C. Palacios, Can we predict the conformational preference of amides? J. Org. Chem. 66 (2001) 7275–7282.
[51] V. Balevicius, Z. Gdaniec, K. Aidas, NMR and DFT study on media effects on proton transfer in hydrogen bonding: concept of molecular probe with an application to ionic and super-polar liquids, Phys. Chem. Chem. Phys. 11 (2009) 8592–8600.
[52] P.A. Rachwal, K.R. Fox, Quadruplex melting, Methods 43 (2007) 291–301.
[53] J.L. Zhou, Y.J. Lu, T.M. Ou, J.M. Zhou, Z.S. Huang, X.F. Zhu, C.J. Du, X.Z. Bu, L. Ma, L.Q. Gu, Y.M. Li, A.S. Chan, Synthesis and evaluation of quindoline derivatives as G-quadruplex inducing and stabilizing ligands and potential inhibitors of telomerase, J. Med. Chem. 48 (2005) 7315–7321.
[54] C.M. Schultes, B. Guyen, J. Cuesta, S. Neidle, Synthesis, biophysical and biological evaluation of 3,6-bis-amidoacridines with extended 9-anilino substituents as potent G-quadruplex-binding telomerase inhibitors, Bioorg. Med. Chem. Lett. 14 (2004) 4347–4351.
[55] A. De Cian, E. Delemos, J.L. Mergny, M.P. Teulade-Fichou, D. Monchaud, Highly efficient G-quadruplex recognition by bisquinolinium compounds, J. Am. Chem. Soc. 129 (2007) 1856–1857.
[56] E.M. Rezler, J. Seenisamy, S. Bashyam, M.Y. Kim, E. White, W.D. Wilson, L.H. Hurley, Telomestatin and diseleno sapphyrin bind selectively to two different forms of the human telomeric G-quadruplex structure, J. Am. Chem. Soc. 127 (2005) 9439–9447.
[57] S. Paramasivan, I. Rujan, P.H. Bolton, Circular dichroism of quadruplex DNAs: applications to structure, cation effects and ligand binding, Methods 43 (2007) 324–331.
[58] O.Y. Fedoroff, M. Salazar, H. Han, V.V. Chemeris, S.M. Kerwin, L.H. Hurley, NMR-Based model of a telomerase-inhibiting compound bound to G-quadruplex DNA, Biochemistry 37 (1998) 12367–12374.
[59] H. Mita, T. Ohyama, Y. Tanaka, Y. Yamamoto, Formation of a complex of 5,10,15,20-tetrakis(N-methylpyridinium-4-yl)-21H,23H-porphyrin with G-quadruplex DNA, Biochemistry 45 (2006) 6765–6772.
[60] M.P. Foster, C.A. McElroy, C.D. Amero, Solution NMR of large molecules and assemblies, Biochemistry 46 (2007) 331–340.
[61] J. Dai, C. Punchihewa, A. Ambrus, D. Chen, R.A. Jones, D. Yang, Structure of the intramolecular human telomeric G-quadruplex in potassium solution: a novel adenine triple formation, Nucleic Acids Res. 35 (2007) 2440–2450.
[62] S. Agrawal, R.P. Ojha, S. Maiti, Energetics of the human Tel-22 quadruplex-telomestatin interaction: a molecular dynamics study, J. Phys. Chem. B. 112 (2008) 6828–6836.
[63] J. Reed, M. Gunaratnam, M. Beltran, A.P. Reszka, R. Vilar, S. Neidle, TRAP-LIG, a modified telomere repeat amplification protocol assay to quantitate telomerase inhibition by small molecules, Anal. Biochem. 380 (2008) 99–105.
[64] A. De Cian, G. Cristofari, P. Reichenbach, E. De Lemos, D. Monchaud, M.P. Teulade-Fichou, K. Shin-Ya, L. Lacroix, J. Lingner, J.L. Mergny, Reevaluation of telomerase inhibition by quadruplex ligands and their mechanisms of action, Proc. Natl. Acad. Sci. U S A 104 (2007) 17347–17352.
[65] E.S. Hwang, Replicative senescence and senescence-like state induced in cancer-derived cells, Mech. Ageing Dev. 123 (2002) 1681–1694.
[66] J.F. Riou, L. Guittat, P. Mailliet, A. Laoui, E. Renou, O. Petitgenet, F. Megnin-Chanet, C. Helene, J.L. Mergny, Cell senescence and telomere shortening induced by a new series of specific G-quadruplex DNA ligands, Proc. Natl. Acad. Sci. U S A 99 (2002) 2672–2677.
[67] A. De Cian, L. Lacroix, C. Douarre, N. Temime-Smaali, C. Trentesaux, J.F. Riou, J.L. Mergny, Targeting telomeres and telomerase, Biochimie 90 (2008) 131–155.
[68] J.M. Zhou, X.F. Zhu, Y.J. Lu, R. Deng, Z.S. Huang, Y.P. Mei, Y. Wang, W.L. Huang, Z.C. Liu, L.Q. Gu, Y.X. Zeng, Senescence and telomere shortening induced by novel potent G-quadruplex interactive agents, quindoline derivatives, in human cancer cell lines, Oncogene 25 (2006) 503–511.
[69] G.M. Morris, D.S. Goodsell, R.S. Halliday, R. Huey, W.E. Hart, R.K. Belew, A.J. Olson, Automated docking using a Lamarckian genetic algorithm and an empirical binding free energy function, J. Comput. Chem. (1998) 1639–1662.
[70] M.F. Sanner, Python: a programming language for software integration and development, J. Mol. Graph Model. 17 (1999) 57–61.